ALBERT-LUDWIGS-
UNIVERSITÄT FREIBURG

MATHEMATISCHE FAKULTÄT

L. Badratinova

Thin-layer effects in a stability problem for equilibrium states between liquid and vapor

Preprint Nr. 26/1998–22.06.1998

MATHEMATISCHE FAKULTÄT · ECKERSTRASSE 1 · 79104 FREIBURG · GERMANY

Thin-layer effects in a stability problem for equilibrium states between liquid and vapor

Lidia Badratinova
Institute of Applied Mathematics, University of Freiburg
Hermann–Herder–Straße 10
Email: lidia@mathematik.uni-freiburg.de

Abstract

The linear nonoscillatory stability of a horizontal vapor layer resting on a heated plate below a layer of its liquid is studied. The liquid is bounded above by a rigid plate that is colder than the lower wall. At the plates, either a heat flux or a temperature is kept constant. The phases are assumed to be incompressible fluids with different physical properties. At their interface, phase change is induced by perturbations, gravity and capillary effects are taken into account. Exact neutral stability conditions are derived, and are examined numerically and in the long-wave approximation. The results show that the arrangement can be linearly stable to nonoscillatory perturbations when both phases are in thin layers. The mechanism of stabilization is described. The stability conditions are formulated in terms of the thickness of the layers and some characteristic length scales.

Keywords. Hydrodynamic stability, liquid-vapor interfaces, Rayleigh–Taylor instability, thin-layer effect, heat transfer

AMS subject classification (1991). 76E10, 76T05, 80A20, 80A22

1 Introduction

A horizontal interface between two motionless incompressible fluids with less dense lower fluid is unstable. The mechanism which tends to deform it is the well-known Rayleigh – Taylor instability (Rayleigh 1900, Taylor 1950). Interaction of this gravity instability with different physical mechanisms have been intensively studied over the past decades (the literature is reviewed in the recent work by Kull 1991). In particular, there have been revealed and described mechanisms that damp and prevent the Rayleigh – Taylor instability.

Renardy (1985) studied the linear stability of plane Cuette flow of two immiscible fluids in two layers. Computing the eigenvalues numerically, she has found that the flow with the more dense fluid on top can be stable if the lower fluid is in a thin layer. The stabilization occurs when the liquid in the thin layer is the less viscous (Renardy 1987). In the Bénard problem where two layers with slightly different physical properties of fluids are bounded by free boundaries, the motionless state with the thin lower layer and the more dense fluid on top can be stabilized when the thermal conductivity of the lower fluid is less than that of the upper one (Renardy 1986). Stabilization due to the effects of stratification for viscosity or thermal conductivity by reducing the thickness of one layer was called the "thin-layer effect" (Hooper 1985, Joseph & Renardy 1992).

Surprising results on interactions between the phase change and gravity mechanisms have been obtained by Busse & Schubert 1971 in their modeling of convecting medium in planetary interiors and atmospheres by two phases with equal viscosities, thermal diffusivities, slightly different densities, and a release of latent heat at the phase separating boundary. Such a univariant phase transition was involved in the Rayleigh – Bénard stability problem. Depending on the temperature gradient field, the influence of the phase change can be stabilizing or destabilizing. A motionless state with the denser phase below and lighter phase above can be unstable while it can be stable with the heavier phase above and the lighter below.

Some kind of thin-layer effect occurs in the model in which the influence of the phase transformation on the Rayleigh – Taylor instability is described for incompressible inviscid fluids with different properties (Hsieh 1972). Assuming a constant temperature difference be held between the rigid boundary plates, Hsieh found that the phase change effect is stabilizing when the vapor is hotter than the liquid. In case of infinitely deep liquid and very thin vapor layer, the growth rate of the Rayleigh – Taylor instability may be greatly reduced at large temperature gradients. Application of Hsieh's results to the problem on film boiling was discussed by Dhir & Lienhard (1972). The film boiling regime is characterized by existence of a vapor layer between heated wall and liquid. At the phase dividing boundary, waves periodically grow and collapse to release bubbles. Dhir & Lienhard have analyzed Hsieh's general dispersion relation for a system at low pressure (the density of the vapor is much less than that of the liquid) and a vapor layer that is not very thin. They showed that no thermal effects did influence the Rayleigh – Taylor instability.

An interesting effect of thin fluid layer was found by Huang & Joseph (1992) in the problem on stability of a motionless liquid-vapor system confined between heated horizontal plates. Both phases are incompressible viscous fluids. Vapor layer lies above and the Rayleigh – Taylor instability does not appear. The plates are at constant temperatures and the upper one, adjacent to the vapor film, is hotter. Analyzing a linear stability problem numerically, Huang & Joseph found an instability arising as overstability. They performed an energy analysis and showed that the instability was due to the phase change occurring at the perturbed interface. With very thick or very thin vapor layer the arrangement was, however, stable.

The effect analogy to that revealed for a very thin vapor layer by Huang & Joseph was found by Badratinova, Colinet, Hennenberg & Legros (1996a, 1996b) and by Badratinova (1996) in problems with a semi-infinite liquid phase being over the vapor layer. The system is heated from the bottom wall which is at a constant temperature or at a constant heat flux. The problem is studied with taking account of the thermocapillary and thermodynamic non-equilibrium effects at the perturbed interface. At the interface, the phases are in thermal equilibrium. The condition of the thermodynamic non-equilibrium is written as the condition of proportionality of the mass flux across the interface to the difference between the chemical potentials of the phases. The cases when the liquid and vapor phases are in the thermodynamic equilibrium with respect to each other (equality of chemical potentials) and when there is no mass transfer across the interface (liquid-gas system) are considered as two limiting cases of the model, corresponding to infinite and zero values of the proportionality coefficient, respectively. The analysis of nonoscillatory perturbations reveals that the gravity mechanism is inactive when the vapor layer is sufficiently thin: in the liquid-gas system, there exists a thermocapillary instability with wave length much less than that of the Rayleigh – Taylor instability, while the rest state of the liquid-vapor system is stable to nonoscillatory perturbations. In both cases, the dominating mechanisms are thermal dissipation in the liquid and viscous dissipation in the lower (gas or vapor) phase.

In the present work, a linear nonoscillatory stability is examined for a rest state of liquid and vapor phases located in layers between two horizontal plates from which the lower plate is hotter

than the upper one. Each plate is kept either at a constant temperature or at a constant heat flux. Hence, the problem is considered for four different thermal boundary conditions for all of which the heat is transferred through the two-layer system from the lower plate to the upper one. The phases are incompressible viscous fluids. The vapor layer lies below the liquid one. Along the interface, the conditions of the thermal and the thermodynamic equilibrium between phases are posed. Effects of thin vapor and of thin liquid layer are studied.

2 Governing Equations and Basic State

In this section the set of governing equations is presented which will be used in the linear stability analysis for the equilibrium state of heated vapor-liquid system. The fluids lie in the (x, z) plane in layers between parallel rigid plates located at $z = -d_1$ and $z = d_2$. Subscripts '1' and '2' will be used respectively for the lower vapor and for the upper liquid phases. The fluids have constant densities ρ_j $(j = 1, 2)$, viscosities η_j (kinematic viscosities $\nu_j = \eta_j/\rho_j$), thermal diffusivities χ_j and thermal conductivities λ_j. The location of the liquid-vapor interface is given by $z - \zeta(x, t) = 0$. In the equilibrium state, the phase interface is defined by the equation $z = 0$ and is at constant saturation temperature T_0. The coefficient of surface tension acting at the interface $z - \zeta(x, t) = 0$ is denoted by σ and assumed to be constant. The velocities are denoted by $\boldsymbol{v}_j$ $(\boldsymbol{v}_j = (u_j, w_j))$, the pressures by p_j and the temperatures by T_j. The two-fluid layer is heated from the lower plate. Four kind of thermal boundary conditions will be considered: the plates $z = -d_1$, $z = d_2$ are kept at different constant temperatures T_{1w}, T_{2w} $(T_{1w} > T_0 > T_{2w})$, the upper plate is kept at a constant temperature T_{1w} $(T_{1w} > T_0)$ and the lower one is at a constant heat flux q, the upper plate is at a constant heat flux q while the lower one is at a constant temperature T_{2w} $(T_{2w} < T_0)$, both plates are kept at a given heat flux q. In fluid j, the equations of incompressibility, of motion and of heat transfer are

$$\nabla \cdot \boldsymbol{v}_j = 0, \tag{1}$$

$$\rho_j \frac{\partial \boldsymbol{v}_j}{\partial t} + (\boldsymbol{v}_j \cdot \nabla)\boldsymbol{v}_j = -\nabla p_j + \eta_j \nabla^2 \boldsymbol{v}_j + \rho_j \boldsymbol{g}, \tag{2}$$

$$\frac{\partial T_j}{\partial t} + \boldsymbol{v}_j \cdot \nabla T_j = \chi_j \nabla^2 T_j. \tag{3}$$

Here $\nabla = (\partial/\partial x, \partial/\partial z)$, $\boldsymbol{g} = (0, -g)$ is the gravity acceleration vector, g is a positive constant.

At the plates, no-slip conditions

$$\boldsymbol{v}_1 = 0 \quad \text{at} \quad z = -d_1, \quad \boldsymbol{v}_2 = 0 \quad \text{at} \quad z = d_2, \tag{4}$$

are given and thermal conditions defined as follows:

$$T_1 = T_{1w}, \quad \text{at} \quad z = -d_1, \quad T_2 = T_{2w}, \quad \text{at} \quad z = d_2 \tag{5a}$$

or

$$-\lambda_1 \partial T_1/\partial z = q \quad \text{at} \quad z = -d_1, \quad T_2 = T_{2w}, \quad \text{at} \quad z = d_2 \tag{5b}$$

or

$$T_1 = T_{1w}, \quad \text{at} \quad z = -d_1, \quad -\lambda_2 \partial T_2/\partial z = q \quad \text{at} \quad z = d_2 \tag{5c}$$

or

$$-\lambda_1 \partial T_1/\partial z = q \quad \text{at} \quad z = -d_1, \quad -\lambda_2 \partial T_2/\partial z = q \quad \text{at} \quad z = d_2. \tag{5d}$$

At the liquid-vapor interface $z = \zeta(x,t)$, the normal mass flux and the tangential component of velocity are continuous, i.e.,

$$\rho_1(\boldsymbol{v}_1 - \boldsymbol{v}_\Sigma)\cdot\boldsymbol{n} = \rho_2(\boldsymbol{v}_2 - \boldsymbol{v}_\Sigma)\cdot\boldsymbol{n}, \quad (\boldsymbol{v}_1 - \boldsymbol{v}_2)\cdot\boldsymbol{\tau} = 0. \tag{6}$$

In addition, normal and tangential momentum and energy fluxes must be also continuous there (Delhaye 1974):

$$(\rho_1(\boldsymbol{v}_1 - \boldsymbol{v}_\Sigma)\cdot\boldsymbol{n})\,(\boldsymbol{v}_1 - \boldsymbol{v}_2)\cdot\boldsymbol{n} + p_2 - p_1 - 2\boldsymbol{n}\cdot(\eta_2\boldsymbol{D}_2 - \eta_1\boldsymbol{D}_1)\boldsymbol{n} = \sigma\nabla\cdot\boldsymbol{n}, \tag{7}$$

$$(\rho_1(\boldsymbol{v}_1 - \boldsymbol{v}_\Sigma)\cdot\boldsymbol{n})\,(\boldsymbol{v}_1 - \boldsymbol{v}_2)\cdot\boldsymbol{\tau} + \boldsymbol{n}\cdot(\eta_2\boldsymbol{D}_2 - \eta_1\boldsymbol{D}_1)\boldsymbol{\tau} = 0, \tag{8}$$

$$\begin{aligned}(\rho_1(\boldsymbol{v}_1 - \boldsymbol{v}_\Sigma)\cdot\boldsymbol{n})\left\{L + \frac{1}{2}\left((\boldsymbol{v}_1 - \boldsymbol{v}_\Sigma)\cdot\boldsymbol{n}\right)^2 - \frac{1}{2}\left((\boldsymbol{v}_2 - \boldsymbol{v}_\Sigma)\cdot\boldsymbol{n}\right)^2\right\}\\ + \lambda_2\nabla T_2\cdot\boldsymbol{n} - \lambda_1\nabla T_1\cdot\boldsymbol{n} \qquad + 2\eta_2(\boldsymbol{D}_2\boldsymbol{n})\cdot(\boldsymbol{v}_2 - \boldsymbol{v}_\Sigma) - 2\eta_1(\boldsymbol{D}_1\boldsymbol{n})\cdot(\boldsymbol{v}_1 - \boldsymbol{v}_\Sigma) = 0.\end{aligned} \tag{9}$$

Here L is the latent heat of vaporization, $\boldsymbol{D}_j = [(\nabla\boldsymbol{v}_j) + (\nabla\boldsymbol{v}_j^T)]/2$ are the rate-of-deformation tensors, $\boldsymbol{n} = (-\zeta_x, 1)(1+\zeta_x^2)^{-1/2}$, $\boldsymbol{\tau} = (1, \zeta_x)(1+\zeta_x^2)^{-1/2}$ are the unit normal and tangent vectors respectively, $\boldsymbol{v}_\Sigma$ is the interface velocity ($\boldsymbol{v}_\Sigma\cdot\boldsymbol{n} = -\zeta_t(1+\zeta_x^2)^{-1/2}$) . A set of interfacial boundary conditions is completed by equality of the temperatures

$$T_1 = T_2 \quad \text{at} \quad z = \zeta(x,t)$$

and of the specific chemical potentials μ_1, μ_2 of the phases

$$\mu_1(T_1, p_1) = \mu_2(T_2, p_2) \quad \text{at} \quad z = \zeta(x,t) \tag{10}$$

which correspondingly express assumptions of the thermal equilibrium and of the thermodynamic quasi-equilibrium between the phases. Equation (10) is written in analogy with the thermodynamic equilibrium condition at a curved equilibrium interface between pure phases (Stephan 1992). In analogy to that case, the local saturation temperature $T_s = T_1 = T_2$ defined by (10) depends on two variables p_1, $p_1 - p_2$ or p_2, $p_1 - p_2$, with a difference of the pressures playing the role of the capillary pressure. Condition (10) will be used in a linearized form. In the basic state, condition (10) is also valid at the phase interface $z = 0$ which is at the thermal equilibrium, e.g. one has the equality $\mu_1(T_0, p_0) = \mu_2(T_0, p_0)$ at $z = 0$ in which p_0 denotes the equilibrium saturation pressure corresponding to the saturation temperature T_0. Linearization of equation (10) near the point (T_0, p_0) gives

$$T_1 = T_2 = T_s = T_0 + \frac{T_0(\rho_2 - \rho_1)}{\rho_2\rho_1 L}(p_1 - p_0) + \frac{T_0}{\rho_2 L}(p_1 - p_2) \quad \text{at} \quad z = \zeta(x,t) \tag{11}$$

(Badratinova, Colinet, Hennenberg & Legros 1996). Formula (11) has been obtained under the assumption that the local thermodynamic quasi-equilibrium takes place everywhere near the moving interface. In other words, near the interface, each of the coexisting phases is assumed to be governed by a Gibbs – Duhem equation, so that the formulas (Prigogine & Defay 1973)

$$\left(\frac{\partial\mu_2}{\partial p}\right)_{T_0,p_0} = \frac{1}{\rho}, \quad \left(\frac{\partial\mu_1}{\partial p}\right)_{T_0,p_0} = \frac{1}{\rho_1}, \quad \left(\frac{\partial\mu_2}{\partial T}\right)_{T_0,p_0} - \left(\frac{\partial\mu_1}{\partial T}\right)_{T_0,p_0} = L/T_0$$

are valid. Note, that if the density of vapor is much less than of liquid, the last term in (11) is small in comparison with the previous one, then equation (11) only slightly differs from the Clausius – Clapeyron relation for vapor phase.

The basic solution of system (1)–(9), (11) can be written as follows

$$\begin{aligned} \boldsymbol{v}_1 = 0, \quad p_1^0 = -\rho_1 g z + p_0, \quad T_1^0 = -\frac{q}{\lambda_1} z + T_0 \quad \text{for} \quad -d_1 < z < 0, \\ \boldsymbol{v}_2 = 0, \quad p_2^0 = -\rho_2 g z + p_0, \quad T_2^0 = -\frac{q}{\lambda_2} z + T_0 \quad \text{for} \quad 0 < z < d_2, \\ \zeta = 0 \end{aligned} \tag{12}$$

Here and everywhere below, q is assumed to be expressed through the corresponding temperature difference if the temperature rather than the heat flux is constant at the wall. In this way we have $q = \lambda_1(T_{1w} - T_0)/d_1 = \lambda_2(T_0 - T_{2w})/d_2$ everywhere in (12) for the boundary condition (5a), q is replaced by $q = \lambda_2(T_0 - T_{2w})/d_2$ only in the formula for T_2^0 for (5b) and it is replaced by $\lambda_1(T_{1w} - T_0)/d_1$ only in the formula for T_1^0 for condition (5c). In the following, the thicknesses d_1, d_2 are assumed to be given. The saturation temperature T_0 is given also. Under these assumptions, a temperature or a heat flux value can be given arbitrarily only on one of the plates. As for a corresponding value in a thermal condition on the other plate, we have to make it agree with the already given one.

3 Neutrally stable perturbations

The governing equations and the boundary conditions are considered now in a dimensionless form. Length is scaled on the vapor film thickness d_1. The scales χ_1/d_1, d_1^2/ν_1, $\rho_1\chi_1\nu_1/d_1^2$, and qd_1/λ_1 are chosen for velocity, time, pressure and temperature respectively. The velocities of fluids are expressed through their stream functions ($u_j = -\partial_z\Psi_j$, $w_j = \partial_z\Psi_j$), the pressures p_j are eliminated and the system is linearized around the basic solution. The functions Ψ_j, T_j, and ζ then represent the perturbations from the state of rest. Assuming the perturbations to be expressed in terms of their normal modes, i.e.,

$$\begin{pmatrix} \Psi_j \\ T_j \\ \zeta \end{pmatrix} = \begin{pmatrix} 0 \\ T_j^0 \\ 0 \end{pmatrix} + \begin{pmatrix} \psi_j(z) \\ i\theta_j(z) \\ ia \end{pmatrix} \exp(nt + ikx),$$

the problem is reduced to an eigenvalue problem in which the growth rate n is the unknown eigenvalue. The consideration is restricted to neutrally stable perturbations, that are modes with zero growth rate. Therefore, n is set equal to zero. The problem then reduces to a boundary value problem for the amplitudes ψ_j, θ_j, a, and the condition for existence of nontrivial solution defines the critical condition for onset of instability to perturbations aperiodic in time. In the boundary value problem, the following dimensionless parameter appear.

$d_0 = d_2/d_1$ relative thickness of the liquid layer

$\rho_* = \rho_1/\rho_2$ density ratio

$\eta_* = \eta_1/\eta_2$ $(\nu_* = \nu_1/\nu_2)$ viscosity (kinematic viscosity) ratio

$\chi_* = \chi_1/\chi_2$ thermal diffusivity ratio

$\lambda_* = \lambda_1/\lambda$ thermal conductivity ratio

$N_g = (\rho_2 - \rho_1)gd_1^2/\sigma$ Bond number

$N_{cr} = \eta_1\chi_1/(\sigma d_1)$ crispation group

$\tau_e = T_0\lambda_1\nu_1/(\rho_1 L^2 d_1^2)$ saturation temperature number

$Q = qd_1/(\rho_1\chi_1 L)$ dimensionless heat flux or temperature difference

The amplitudes of the stream functions satisfy the equations ($D := d/dz$)

$$(D^2 - k^2)^2\psi_1 = 0 \quad \text{for} \quad -1 < z < 0, \quad (D^2 - k^2)^2\psi_2 = 0 \quad \text{for} \quad 0 < z < d_0 \tag{13}$$

with the no-slip boundary conditions

$$\psi_1 = D\psi_1 = 0 \quad \text{at} \quad z = -1, \quad \psi_2 = D\psi_2 = 0 \quad \text{at} \quad z = d_0 \tag{14}$$

and the continuity conditions for the tangential component of velocity, mass flux, and for the two components of momentum, valid at $z = 0$

$$\begin{gathered} D\psi_1 = D\psi_2, \quad \psi_2 = \rho_*\psi_1, \\ 3(1 - \eta_*^{-1})k^2 D\psi_2 + \eta_*^{-1}D^3\psi_2 - D^3\psi_1 + k(k^2 - N_g)N_{cr}^{-1}a = 0, \\ \eta_*^{-1}(D^2 + k^2)\psi_2 = (D^2 + k^2)\psi_1. \end{gathered} \tag{15}$$

The equations for amplitudes of temperature perturbation are

$$\begin{gathered} (D^2 - k^2)\theta_1 = -k\psi_1 \quad (-1 < z < 0), \\ (D^2 - k^2)\theta_2 = -\chi_*\lambda_* k\psi_2 \quad (0 < z < d_0). \end{gathered} \tag{16}$$

The respective boundary conditions to be considered are

$$\theta_1 = 0 \quad \text{at} \quad z = -1, \quad \theta_2 = 0 \quad \text{at} \quad z = d_0 \tag{17a}$$

or

$$D\theta_1 = 0 \quad \text{at} \quad z = -1, \quad \theta_2 = 0 \quad \text{at} \quad z = d_0 \tag{17b}$$

or

$$\theta_1 = 0 \quad \text{at} \quad z = -1, \quad D\theta_2 = 0 \quad \text{at} \quad z = d_0 \tag{17c}$$

or

$$D\theta_1 = 0 \quad \text{at} \quad z = -1, \quad D\theta_2 = 0 \quad \text{at} \quad z = d_0. \tag{17d}$$

At the interface $z = 0$, the temperature continuity and the jump balance of energy yield

$$\theta_1 = \theta_2 + (1 - \lambda_*)a, \quad Q(D\theta_1 - \lambda_*^{-1}D\theta_2) = k\psi_1. \tag{18}$$

Here, we find also the x-derivative of the interfacial temperature and make it equal to the gradient of the saturation temperature. As the pressures are expressed through the stream functions, this yields

$$Qk(\theta_2 - \lambda_* a) = \tau_e D[D^2\psi_1 - \nu_*^{-1}D^2\psi_2 - k^2(1 - \nu_*^{-1})\psi_2]. \tag{19}$$

4 Conditions for onset of instability

The system of equations (13) to (19) is solved analytically. To present the solution, introduce first the functions

$$\begin{aligned} &f_1(\xi) = \xi^2/(\sinh^2\xi - \xi^2), \qquad f_2^{\pm}(\xi) = (\xi \pm \sinh\xi\cosh\xi)/(\sinh^2\xi - \xi^2), \\ &f_3(\xi) = (\sinh^3\xi - \xi^3\cosh\xi)/(\sinh\xi(\sinh^2\xi - \xi^2)), \\ &f_4(\xi) = 1 + \xi(2\xi - (2 + \xi^2)\tanh\xi)/(\sinh^2\xi - \xi^2) \end{aligned} \tag{20}$$

which will appear either as functions of k or as functions of $k_0 = kd_0$. Note, that

$$k = \alpha d_1, \quad k_0 = kd_0 = \alpha d_2,$$

where α is a dimensional wave number. Introduce also the following notations

$$f_i = f_i(k), \quad f_{i0} = f_{i0}(k_0), \quad i = 1, 3, 4; \quad f_2^{\pm} = f_2^{\pm}(k), \quad f_{20}^{\pm} = f_2^{\pm}(k_0)$$

and functions

$$r = r(k, k_0) = -(f_1/f_2^-)(1 - \nu_*^{-1} f_{10}/f_1)(1 + \eta_*^{-1} f_{20}^-/f_2^-)^{-1}, \tag{21}$$

$$G(k, k_0) = (\eta_*^{-1} f_{10} - f_1)r + \nu_*^{-1} f_{20}^+ + f_2^+. \tag{22}$$

Then, the solution to equations (13)–(15) can be written as

$$\psi_1 = a\frac{N_g - k^2}{2k^2 N_{cr} G(k, k_0)}[L_1(kz)\cosh kz + L_2(kz)\sinh kz],$$

$$\psi_2 = a\frac{N_g - k^2}{2k^2 N_{cr} G(k, k_0)}[L_3(kz)\cosh kz + L_4(kz)\sinh kz] \tag{23}$$

where $L_i(kz)$ are the linear functions in kz presented in Appendix A. The solution of the temperature equations (16) leads to the following. In the case of the boundary conditions (17a), (18) or (17b), (18) where the upper wall is at a constant temperature, expressions for the temperature can be written in the form

$$\theta_1 = (C - \lambda_* a)(\cosh kz - \lambda_*^{-1}\coth k_0 \sinh kz) + A[P_3(kz)\cosh kz + P_{4T}(kz)\sinh kz],$$

$$\theta_2 = C(\cosh kz - \coth k_0 \sinh kz) + A[P_1(kz)\cosh kz + P_{2T}(kz)\sinh kz], \tag{24}$$

where

$$A = a\frac{N_g - k^2}{2k^2 N_{cr} G(k, k_0)}$$

is the amplitude of perturbation to the stream functions (see (23)), P_1, P_{2T}, P_3 and P_{4T} are the second order polynomials in kz written in Appendix A.

In (24), the coefficient C is defined by

$$C = a\lambda_* - a\frac{[F^{TT}(k, k_0) + 4kQ^{-1}](k^2 - N_g) + 8N_{cr}k^3 G(k, k_0)(\coth k + \coth k_0)}{8k^3 N_{cr} G(k, k_0)(\coth k + \lambda_*^{-1}\coth k_0)} \tag{25}$$

when the lower plate has a fixed temperature, i.e. (17a) applies. For condition (17b), where the lower plate has a fixed heat flux, C has found to be

$$C = a\lambda_* - a\frac{[F^{qT}(k, k_0) + 4kQ^{-1}](k^2 - N_g) + 8N_{cr}k^3 G(k, k_0)(\tanh k + \coth k_0)}{8k^3 N_{cr} G(k, k_0)(\tanh k + \lambda_*^{-1}\coth k_0)}. \tag{26}$$

Here

$$F^{TT}(k, k_0) = (\chi_* f_{30} - f_3)r + \chi_*\rho_*(3\coth k_0 - k_0 f_{10}) + 3\coth k - k f_1, \tag{27}$$

$$F^{qT}(k, k_0) = (\chi_* f_{30} - f_4)r + \chi_*\rho_*(3\coth k_0 - k_0 f_{10}) + (f_3 + 2)\tanh k. \tag{28}$$

Further, when the upper wall is at a constant heat flux, equation (16) is considered with conditions (17c), (18) or (17d), (18). The solution is

$$\theta_1 = (C - \lambda_* a)(\cosh kz - \lambda_*^{-1}\tanh k_0 \sinh kz) + A[P_3(kz)\cosh kz + P_{4q}(kz)\sinh kz],$$

$$\theta_2 = C(\cosh kz - \tanh k_0 \sinh kz) + A[P_1(kz)\cosh kz + P_{2q}(kz)\sinh kz]. \tag{29}$$

Expressions for the polynomials P_{2q} and P_{4q} are presented in Appendix A. In the case of an isothermal lower plate, the coefficient C is given by

$$C = a\lambda_* - a\frac{[F^{Tq}(k,k_0) + 4kQ^{-1}](k^2 - N_g) + 8N_{cr}k^3G(k,k_0)(\coth k + \tanh k_0)}{8k^3N_{cr}G(k,k_0)(\coth k + \lambda_*^{-1}\tanh k_0)} \tag{30}$$

while in the case the lower plate is at a fixed heat flux we have

$$C = a\lambda_* + a\frac{[F^{qq}(k,k_0) + 4kQ^{-1}](k^2 - N_g) + 8N_{cr}k^3G(k,k_0)(\tanh k + \tanh k_0)}{8k^3N_{cr}G(k,k_0)(\tanh k + \lambda_*^{-1}\tanh k_0)}, \tag{31}$$

where

$$F^{Tq}(k,k_0) = (\chi_* f_{40} - f_3)r + \chi_*\rho_*(f_{30} + 2)\tanh k_0 + 3\coth k - kf_1, \tag{32}$$

$$F^{qq}(k,k_0) = (\chi_* f_{40} - f_4)r + \chi_*\rho_*(f_{30} + 2)\tanh k_0 + (f_3 + 2)\tanh k. \tag{33}$$

To get the conditions for onset of the nonoscillatory instability, we use the interface condition (19). The right-hand side is calculated with the help of (23). For the left-hand side, we find from (24), (29) that $\theta_2 = C$ at $z = 0$. Using expressions (25), (26), (30), (31), we obtain the critical dependence $Q(k)$ at which the nonoscillatory instability occurs. This dependence is ($k_0 = kd_0$) :

$$Q = Q^{TT}(k) = -\frac{4(k^2 - N_g)[\tau_e(\coth k + \lambda_*^{-1}\coth k_0)H(k,k_0) + k]}{F^{TT}(k,k_0)(k^2 - N_g) + 8N_{cr}k^3G(k,k_0)(\coth k + \coth k_0)} \tag{34}$$

for the case of two isothermal plates,

$$Q = Q^{qT}(k) = -\frac{4(k^2 - N_g)[\tau_e(\tanh k + \lambda_*^{-1}\coth k_0)H(k,k_0) + k]}{F^{qT}(k,k_0)(k^2 - N_g) + 8N_{cr}k^3G(k,k_0)(\tanh k + \coth k_0)} \tag{35}$$

for the case where the low plate is at a constant heat flux and the upper is isothermal,

$$Q = Q^{Tq}(k) = -\frac{4(k^2 - N_g)[\tau_e(\coth k + \lambda_*^{-1}\tanh k_0)H(k,k_0) + k]}{F^{Tq}(k,k_0)(k^2 - N_g) + 8N_{cr}k^3G(k,k_0)(\coth k + \tanh k_0)} \tag{36}$$

if isothermal is the low plate and at a constant heat flux is the upper one, and

$$Q = Q^{qq}(k) = -\frac{4(k^2 - N_g)[\tau_e(\tanh k + \lambda_*^{-1}\tanh k_0)H(k,k_0) + k]}{F^{qq}(k,k_0)(k^2 - N_g) + 8N_{cr}k^3G(k,k_0)(\tanh k + \tanh k_0)} \tag{37}$$

if both plates are at a given heat flux. In (34)–(37), the following notation

$$H(k,k_0) = 2k^3[(\nu_*^{-1} - 1 + \nu_*^{-1}f_{10} - f_1)r + f_2^+ + \nu_*^{-1}\rho_* f_{20}^+] \tag{38}$$

has been introduced. To discuss the physical meaning of the terms appearing in formulas (34)–(37), we note first that in the key equation (19) the perturbation to the interface temperature, which is $Q(\theta_2 - \lambda_* a) = Q(C - \lambda_* a)$, is not proportional to Q. That is seen from expressions (25), (26), (30), (31) whose right-hand sides contain terms proportional to Q^{-1}. These terms, appearing due to discontinuity of the heat flux at the phase change interface (see eq. (18)), reflect influence of the effect of latent heat release on the interface temperature. In formulas (34)–(37), responsible for this effect are the terms $4(k^2 - N_g)k$ in the numerator. The denominator is, therefore, not proportional to the perturbation of the total surface temperature. Its first term represents the contribution to the temperature perturbation which is due to the effect of convection occurring in the contacting layers and associated with gravity waves. This can be recognized with the help of equation (23) showing that the amplitude of the stream functions is proportional to $k^2 - N_g$. The

second term proportional to N_{cr} reflects the perturbation of the surface temperature which is due to the effect of interface perturbation. In each formula for the critical Q, the numerator contains a term proportional to τ_e. This term appears because the saturation temperature changes due to disturbances of the interface.

Note also, that the equations (34)–(37) contain functions which are described by (22), (27), (28), (32), (33), (38) in terms of the function r defined by (21). The formula $r = \psi_{1z}/(k\psi_1)|_{z=0}$ can shown to be valid. It shows that r is proportional to the ratio between the tangential and normal components for the vapor velocity at the interface.

In order to examine the relative importance of the described effects, an analysis of conditions (34)–(37) will be made in the limiting case of short wavelength and in the following three cases: the vapor is in a thin layer, the liquid is in a thin layer, both fluids are in thin layers of equal thickness. The analysis will be accompanied by numerical examples. As a test fluid to which the results shall be applied, water with its vapor at $373K$ shall be used. For this system, the physical parameters are:

$$\rho_1 = 6 \times 10^{-4}\, g/cm^3 \qquad \rho_2 = 0.965\, g/cm$$
$$\nu_1 = 0.208\, cm^2/s \qquad \nu_2 = 0.0029\, cm^2/s$$
$$\chi_1 = 0.2\, cm^2/s \qquad \chi_2 = 1.685 \times 10^{-3}\, cm^2/s$$
$$\lambda_1 = 2.39 \times 10^3\, erg/(cm\, s\, K) \qquad \lambda_2 = 6.8 \times 10^4\, erg/(cm\, s\, K)$$
$$L = 2.26 \times 10^{10}\, erg/g \qquad \sigma = 59.9\, dynes/cm.$$

Note finally that, at $Q = 0$, equations (34)–(37) give one and the same condition: $k = k_c = \sqrt{N_g}$. In dimensional form, this condition is expressed by the equality $\alpha = \alpha_c = \sqrt{(\rho - \rho_1)g/\sigma}$ which is well-known in the theory of the Rayleigh – Taylor instability (see Chandrasekhar 1961). The critical wave-number α_c, determines the instability interval $(0, \alpha_c)$ for a resting state of two horizontal layers of isothermal immiscible inviscid fluids of constant density, from which the lower one is the less dense. The perturbations with the wave number $\alpha > \alpha_c$ are stabilized by surface tension. In Chandrasekhar (1961), the case of two viscous semi-infinite fluids has been considered also. It was shown that the instability interval is independent of viscosity. Below, in appendix B, we show that such an independence takes place also in the case where only one fluid is semi-infinite and the other is in a thin layer.

It is known that the problem on the Rayleigh – Taylor instability vanishes in the marginal case of zero growth rate: $n = 0$. That is because it follows from the kinematic condition that the amplitude a of surface wave is inversely proportional to n (see Appendix B). Strictly speaking, in order to examine how gravity interacts with other effects, one always has to study oscillatory modes. However, when examining the dispersion relations for the Rayleigh – Taylor instability of viscous fluids, one finds that if one formally puts here $n = 0$, then one obtains, as a solution, the critical wave number α_c (see Chandrasekhar 1961 and Appendix B).

In the problem under consideration, the case $Q = 0$ corresponds to the case of two isothermal fluids. If $Q = \tau_e = 0$, equations (34)–(37) take the form $4(N_g - k^2)k = 0$, expressing the immiscibility condition: $\psi_1 = 0$ at $z = 0$. Hence, the critical wave number $k_c = \sqrt{N_g}$ should be a solution to the dispersion relation for hydrodynamic problem (13)–(15) with $\psi_1 = 0$ at $z = 0$. Therefore, we may conclude that for $Q = 0$, the condition of instability is defined by $k < k_c = \sqrt{N_g}$. In Appendix B it is shown that all perturbations with wave numbers belonging to the instability interval $(0, k_c)$ grow monotonically. This is also expected to be the case for arrangements with two finite layers. In the following analysis for non-isothermal cases, if the instability to nonoscillatory

perturbations exists, we shall compare the instability interval with the interval of the Rayleigh – Taylor instability $0 < k < k_c$.

5 About short waves

To examine a short wave approximation to conditions (34)÷(37), we note first that the leading order approximations to the functions defined by (20) at the limit $\xi \to \infty$ are $f_1 \sim 0$, $f_2^{\pm} \sim \pm 1$, $f_3 \sim 0$, $f_4 \sim 1$. Using this formulas, we find from (21) that $r \sim 0$ as $k \to \infty, k_0 \to \infty$. (This means that transport of mass in the transverse direction is negligibly small in comparison with the mass transfer across the interface). Further, at the limit under consideration, $G \sim 1 + \nu_*^{-1}$, $H \sim 2k^3(1 + \nu_*^{-1}\rho_*)$, and all functions defined by (27), (28), (32), (33) have the same approximation $\sim 3(\chi_*\rho_* + 1)$. From this it follows that all four equations (34)–(37) take the same form

$$Q \sim -\frac{4k[2\tau_e(1+\lambda_*^{-1})(1+\rho_*\nu_*^{-1})k^2+1]}{3(\chi_*\rho_*+1)+16kN_{cr}(1+\nu_*^{-1})}. \tag{39}$$

We shall show now that the short-wave approximation cannot be realized for physically realistic temperature gradients across the system. It seems, that the dominating terms in (39) are those representing the effects of saturation temperature perturbation and of surface deformation. However, we compare the two terms in the numerator of (39) and find that the first term is larger than the second one if $\alpha > \alpha^* = \rho_1^{1/2}L/[2T_0\lambda_1\nu_1(1+\lambda_*^{-1})(1+\rho_*\nu_*^{-1})]^{1/2}$. Analogously, we find that the second term in the denominator becomes larger than the first one for $\alpha > \alpha^{**} = 3\sigma/(16\eta_1\chi_1)$. For water system at $373K$, to the values α^*, α^{**} there correspond wavelengths that are respectively equal to $10^{-6}cm$ and $2 \times 10^{-6}cm$. For the wavelength equal to $10^{-6}cm$, we calculate from (39) the vertical temperature gradient in the vapor q/λ_1 and find that it is equal to $6.1 \times 10^9\, K/cm$! If one neglects in (39) the first term in the numerator and the second term in the denominator, then the parameter Q is proportional to the wave number k. For short waves, Q is large. Even for the wavelength equal to $1cm$, equation (39) leads to the critical value $q/\lambda_1 = 9000\, K/cm$ which is large to be considered as physically realistic. Therefore, the analysis of short waves predicts that the depth of the fluids is an important factor affecting the stability to nonoscillatory perturbations.

6 Long-wave asymptotics, numerical samples

Thin vapor layer

Let both phases be of finite depth. Let also the depth of the vapor be small compared to that of the liquid phase: $d_1 \ll d_2$. Equations (34)–(37) will be examined now in such a long-wave limit where $k \to 0$, $k_0 \to 0$, but $k_0 \gg k$. Here, the inequality $k_0 \gg k$ is equivalent to the above assumption $d_1 \ll d_2$ ($d_0 \gg 1$). In order to get a first-order approximation to each term in equations (34)–(37), we use for (21) the following asymptotic expressions $f_1(\xi) \sim 3/\xi^2 - 2/5$, $f_2^+(\xi) \sim 6/\xi^3$, $f_2^-(\xi) \sim -2/\xi$, $f_3(\xi) \sim \xi^2/5$, $f_4(\xi) \sim \xi^2/3$. We use also $\coth\xi \sim 1/\xi + \xi/3$. Further, taking into account order of magnitudes of the physical parameters in the test system "water- steam at $373K$", we assume that

$$\rho_* < 1, \quad \eta_* d_0 = O(1) \quad (\text{or} \quad \eta_* d_0 \gg 1), \quad \chi_* d_0^2 \gg 1.$$

Then, we get the approximations

$$r \sim \frac{3}{2k(1+\eta_*^{-1}d_0^{-1})}, \quad G \sim \frac{3(1+4\eta_*^{-1}d_0^{-1})}{2k^3(1+\eta_*^{-1}d_0^{-1})}, \quad H \sim \frac{3(1+4\eta_*^{-1}d_0^{-1})}{1+\eta_*^{-1}d_0^{-1}},$$

$$F^{TT} = F^{qT} \sim \frac{3\chi_* d_0^2 k}{10(1+\eta_*^{-1}d_0^{-1})}, \quad F^{Tq} = F^{qq} \sim \frac{\chi_* d_0^2 k}{2(1+\eta_*^{-1}d_0^{-1})}. \quad (40)$$

Using (40), under the assumption $N_g \ll 1$, we reduce the marginal nonoscillatory stability conditions (34)-(37) to the following approximate forms

$$Q = Q^{TT}(k) = -\frac{40(k^2 - N_g)[3\tau_e(1+\lambda_*^{-1}d_0^{-1})(1+4\eta_*^{-1}d_0^{-1}) + k^2(1+\eta_*^{-1}d_0^{-1})]}{3\chi_* d_0^2\,[k^4 - N_g k^2 + 40N_{cr}\chi_*^{-1}d_0^{-2}(1+4\eta_*^{-1}d_0^{-1})]} \quad (41)$$

for the case of two isothermal plates,

$$Q = Q^{qT}(k) = -\frac{40(k^2 - N_g)[3\tau_e(k^2+\lambda_*^{-1}d_0^{-1})(1+4\eta_*^{-1}d_0^{-1}) + k^2(1+\eta_*^{-1}d_0^{-1})]}{3\chi_* d_0^2\,[k^4 - N_g k^2 + 40N_{cr}\chi_*^{-1}d_0^{-3}(1+4\eta_*^{-1}d_0^{-1})]} \quad (42)$$

when the lower plate is at a constant heat flux and the upper one is isothermal,

$$Q = Q^{Tq}(k) = -\frac{8(k^2 - N_g)[3\tau_e(1+\lambda_*^{-1}d_0 k^2)(1+4\eta_*^{-1}d_0^{-1}) + k^2(1+\eta_*^{-1}d_0^{-1})]}{\chi_* d_0^2\,[k^4 - N_g k^2 + 24N_{cr}\chi_*^{-1}d_0^{-2}(1+4\eta_*^{-1}d_0^{-1})]} \quad (43)$$

if the lower plate is isothermal and the upper is at a given heat flux,

$$Q = Q^{qq}(k) = -\frac{8(k^2 - N_g)[3\tau_e(1+\lambda_*^{-1}d_0)(1+4\eta_*^{-1}d_0^{-1}) + 1 + \eta_*^{-1}d_0^{-1}]}{\chi_* d_0^2\,[k^2 - N_g + 24N_{cr}\chi_*^{-1}d_0^{-1}(1+4\eta_*^{-1}d_0^{-1})]} \quad (44)$$

if both phases are at a given heat flux. Note that the Bond number can be presented as $N_g = (d_1/l_{ca})^2$ where $l_{ca} = \sqrt{\sigma/[(\rho_2 - \rho_1)g]}$ is the capillary length. The condition $N_g \ll 1$ is, therefore, equivalent to the requirement $d_1 \ll l_{ca}$.

Consider first equation (41). When $k > \sqrt{N_g}$, both the numerator and the denominator are positive, and the function $Q^{TT}(k)$ is negative, i.e. the neutral stability curve $Q = Q^{TT}(k)$ lies in the negative half-plane $Q < 0$. Also, one readily obtains that $Q^{TT}(0) = \tau_e N_g(1+\lambda_*^{-1}d_0^{-1})/N_{cr} > 0$ and $Q^{TT}(\sqrt{N_g}) = 0$.

Let $0 < k < \sqrt{N_g}$. The numerator is now negative. The denominator, which is a second order polynomial in k^2, can be shown to allow no real roots and be positive when

$$(d_1/\delta_T)^3(d_2/l_{ca})^2 < 160(1+4\eta_*^{-1}d_0^{-1}), \quad (45)$$

where

$$\delta_T = \frac{\eta_1^{1/3}\chi_2^{1/3}}{[(\rho_2 - \rho_1)g]^{1/3}} \quad (46)$$

is a characteristic length which characterizes the vapor layer thickness at which the effects of vapor viscosity and of liquid heat diffusivity are as important as the gravity effect. Thus, under the validity of (45), the function $Q^{TT}(k)$ is positive and the neutral stability curve lies in the positive half-plane $Q > 0$.

Such a situation is presented in figure 1 plotted with the help of equation (34). The dot-dashed curve represents the long-wave approximation. This figure is based on dimensionless parameters which correspond to the case where the water layer has the thickness $d_2 = 0.16\,cm$ and the thickness of the vapor layer is $d_1 = 3.6 \times 10^{-3}\,cm$. Note that, for the water system at the earth gravity acceleration, $\delta_T = 6 \times 10^{-4}\,cm$, $l_{ca} = 0.252\,cm$ and the critical wavelength $l_c = 2\pi l_{ca}$, corresponding to the critical wave number $k_c = \sqrt{N_g}$ of the Rayleigh-Taylor instability, is equal to $1.58\,cm$. Hence, $d_1 = 6\delta_T$ and the value of d_2 is approximately ten times less than the value of l_c. From figure 1, it is seen that the long-wave approximation (41) describes well the behavior

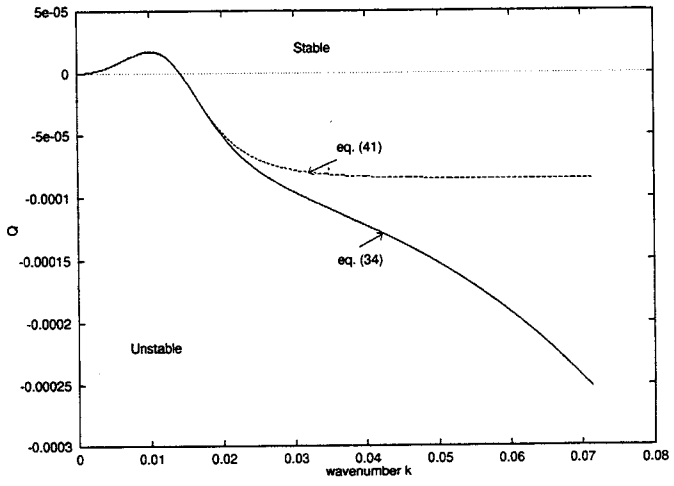

Figure 1: Neutral stability curve when both plates are isothermal, $d_1 = 3.6 \times 10^{-3}\, cm$, $d_0 = 44.44$, $N_g = 2 \times 10^{-4}$, $N_{cr} = 1.2 \times 10^{-4}$, $\tau_e = 4.7 \times 10^{-8}$, $\rho_* = 6.2 \times 10^{-4}$, $\eta_* = 0.045$, $\chi_* = 118.69$, $\lambda_* = 0.035$. The dashed curve represents the long-wave approximation.

of the neutral stability curve inside the interval $(0, \sqrt{N_g})$ as well as in a vicinity of this interval. (The discrepancy occurring at $k \approx 0.02$ is explained by the fact that to $k = 0.02$ there corresponds the value $k_0 = 0.9$ which is not small in comparison with unity.) Since at $Q = 0$ the instability interval is $(0, \sqrt{N_g})$, and since this instability interval should belong to the domain of instability, we conclude that the arrangement is unstable for all points (k, Q) lying below the neutral curve. In the domain above the neutral curve, the arrangement is stable. Figure 1 shows that, with large positive Q, the arrangement is linearly stable to all monotonic perturbations. Namely, the stability takes place when the value of Q is larger then the maximal value $Q^{TT}_{max} = 1.7 \times 10^{-5}$ reached by the function Q^{TT} at $k = k_m = 0.01$. To the value Q^{TT}_{max} corresponds the temperature difference: $T_{1w} - T_0 = 0.015K$.

Let $0 < k < \sqrt{N_g}$, but condition (45) be not satisfied. Then, the denominator of (41) can be shown to allow the two positive roots k_1^{TT}, k_2^{TT} defined by

$$k^{TT}_{1,2} = \left(\frac{N_g}{2}\right)^{1/2} \left[1 \mp \sqrt{1 - 160(1 + 4\eta_*^{-1} d_0^{-1})(\frac{l_{ca}}{d_2}^2)(\frac{\delta_T}{d_1}^3)}\right]^{1/2} . \tag{47}$$

For $0 < k < k_1^{TT}$ and for $k_2^{TT} < k < \sqrt{N_g}$, the denominator is positive, and it is negative when $k_1^{TT} < k < k_2^{TT}$. We expect thus existence of two asymptotes $k = k_1^{TT}$ and $k = k_2^{TT}$ in the picture of the neutral stability plotted in the plane (k, Q). This is seen in figure 2 to which correspond the following depths: $d_1 = 15\delta_{1T} = 0.009\, cm$, $d_2 = 0.16 cm$. There exist three neutral stability curves dividing the plane (k, Q) into four domains. The asymptotes are not plotted, but their existence is evident. The instability takes place in the only domain, this is that one to which the interval $(0, \sqrt{N_g})$ of the Rayleigh-Taylor instability belongs. In the case under consideration Q is positive. As is seen from figure 2 , with large values of Q, the instability takes place in the interval (k_1^{TT}, k_2^{TT}) which length is about two times less than that for the interval of the Rayleigh-Taylor instability. Very long waves are stable. With the help of figures 1 and 2, it was shown that stability may hold also to perturbations with $k < \sqrt{N_g}$, which are not expected to be stabilized by surface

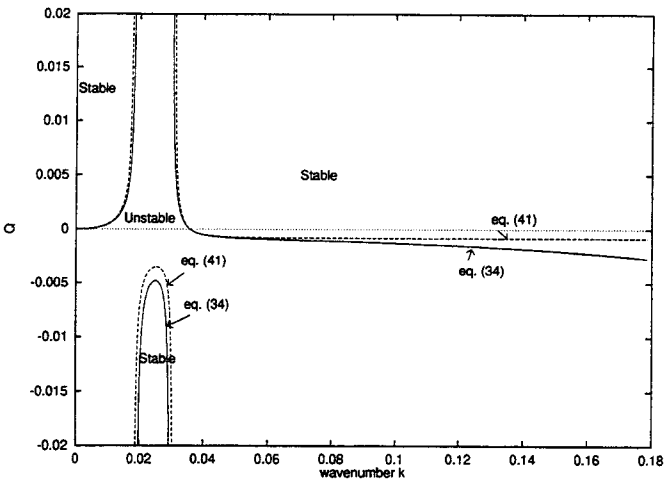

Figure 2: Neutral stability curves when both plates are isothermal, $d_1 = 9 \times 10^{-3}\, cm$, $d_0 = 17.78$, $N_g = 1.28 \times 10^{-3}$, $N_{cr} = 4.6 \times 10^{-5}$, $\tau_e = 7.5 \times 10^{-9}$. The parameters ρ_*, η_*, χ_*, λ_* have the same values as for figure 1. The dashed curves represent the long-wave approximation.

tension. We must, therefore, describe the mechanism which underlies such a stability. With high positive Q, the stability condition is independent of Q : in the case presented in figure 1 it is described by (45), and in the case shown in figure 2 it is given by the inequality $k < k_1^{TT}$ with k_1^{TT} determined in (47). In both cases, the condition of stability is described in terms of the thickness δ_T. This is more clearly seen when η_2 is set equal to zero and the depth d_2 is assumed to be fixed. In the first case, the stability condition (45) yields: $d_1 < 160^{1/3}\delta_T(l_{ca}/d_2)^{2/3}$. In the second case, from (47) it follows that the maximal length of the stability interval, equal to $(N_g/2)^{1/2}$, is reached when $d_1 = 160^{1/3}\delta_T(l_{ca}/d_2)^{2/3}$. For $d_1 > 160^{1/3}\delta_T(l_{ca}/d_2)^{2/3}$, increasing d_1 leads to decrease of the width of the stability interval and, for $d_1 \gg 160^{1/3}\delta_T(l_{ca}/d_2)^{2/3}$, the instability takes place already in the whole interval $(0, \sqrt{N_g})$. If δ_T is equal to zero, there is no stability. The stabilizing effects are, therefore, those represented in the numerator of expression (46) for δ_T : the vapor viscosity and liquid heat diffusivity. However, the mechanism that underlies the stability is the effect of the phase change.

To explain this, note that, in equations (41)–(44), the viscosity and diffusivity effects are presented in the last term of the denominator, which reflects the contribution of surface deformation. These two effects play a stabilizing role, because the last term is positive. We examined also the stability problem when the phase change is absent (liquid-gas system). We have taken into account the thermocapillarity and found that the term expressing the surface deformation effect had negative sign and that, in absence of the phase change, the effect of gas viscosity and of liquid heat diffusivity led to extension of the instability interval in comparison with the interval $(0, \sqrt{N_g})$ of the Rayleigh-Taylor instability. Note, that the problem on the thermocapillary instability is determined by equations (13) - (18) in which one has to put $\psi_1 = 0$ at $z = 0$ and to take into account the thermocapillary effect in the last equation (15). When the last equation (15) (used now as the key equation to derive the neutral stability condition) is omitted, the solution to the problem the modified problem (13) - (18) is determined by expressions following from (22)-(33) "in the limit where the ratio r of tangential to normal component of velocity at $z = 0$ tends to infinity". More precisely, in all functions depending on r, only terms proportional to r have to be conserved. In

particular, the function $G(k, k_0)$ defined by (22) has to be replaced by $\eta_*^{-1} f_{10} - f_1$. In the limit $k \to 0$, $k_0 \to 0$ ($k_0 \gg k$, the function $G(k, k_0)$ behaves asymptotically as $-3/k^2$, i.e., it has the negative sign, which is opposite to the sign of the asymptotic approximation to $G(k, k_0)$ (see (40)) in the case of liquid-vapor system. As is seen from comparison of the neutral stability conditions (41) - (44) with the original equations (34) - (37), the sign of the last term in the denominator of expressions (41) - (44) is determined by the sign of the function $G(k, k_0)$.

In the described mechanism, the absolute linear stability to nonoscillatory perturbations is possible only in the arrangement with a very thin vapor layer. When $d_2 \sim l_{ca}$, the thickness of the vapor layer should not be very large in comparison with the thickness δ_T defined by (46). One can say that, if the thickness of the liquid layer is measured by the capillary length l_{ca}, then, to formulate the condition for stability, the vapor layer thickness should be measured by the length δ_T. In (45), the parameter $\eta_*^{-1} d_0^{-1}$ represents influence of the liquid viscosity. This parameter, depending on the vapor depth, can be expressed through the lengths l_{ca}, δ_T as follows:

$$\eta_*^{-1} d_0^{-1} = V_T (d_1/\delta_T)(l_{ca}/d_2), \tag{48}$$

where V_T is a parameter representing the effect of the liquid viscosity, which is defined by

$$V_T = \frac{\eta_2}{\eta_1} \frac{\delta_T}{l_{ca}} = \frac{\eta_2 \chi_2^{1/3} [(\rho_2 - \rho_1) g]^{1/6}}{\eta_1^{2/3} \sigma^{1/2}}. \tag{49}$$

For $d_2 \sim l_{ca}$, numerical calculations show that, in the case with one neutral stability curve, such as presented in figure 1, the value of Q_{max}^{TT} is well predicted by the long-wave approximation for all values of d_1, which are not very close to the critical value at which inequality (45) already fails (e.g., the denominator of (41) changes sign). In figure 3, a comparison is made for the curves determined by equations (34) and (41). Here, the value of d_2 is the same as for figure 1, but $d_1 = 13\delta_T$. The value of d_1, equal to 7.8×10^{-3} cm, only slightly differs from the value 8.2×10^{-3} cm for which it was found that (34) determines already three neutral stability curves. It is seen that, for Q, the long-wave approximation predicts a maximal value being 2.5 times larger than the value obtained from exact equation (34). The discrepancy can be explained by the fact that, in the denominator of (41), neglected terms of order k^6 become important. Let $d_1 \ll d_2 \ll l_{ca}$. Estimate the left-hand side of (45). Let, for instance, $d_2 \sim l_{ca}/10$, $d_1 \sim l_{ca}/100$. Then, one has $(d_1/\delta_T)^3 (d_2/l_{ca})^2 \sim 10^{-8} (l_{ca}/\delta_T)^3 \approx 1.8$. Hence, inequality (45) "effectively" holds, i.e. /, the left-hand side is much less than the right-hand side. When $d_1 \ll d_2 \ll l_{ca}$ or $d_1 \ll d_2 \sim l_{ca}$ and (45) "effectively" holds, the values of Q_{max}^{TT} are well predicted by the long-wave approximation (41), and it is possible to find an approximate formula for Q_{max}^{TT}. To do this, note that, in the numerator of the right-hand side of (41), the first term in the square brackets is much less then the second one if $k \gg k^* = 3^{1/2} \tau_e^{1/2} (1 + \lambda_*^{-1} d_0^{-1})^{1/2} (1 + 3/(1 + \eta_* d_0))^{1/2}$. For the water system with the parameters as in figure 1, $k^* = 6.8 \times 10^{-4}$, $k_m = 10^{-2}$, so that $k_m \gg k^*$, and, at $k = k_m$, the term proportional to τ_e gives a small contribution. Neglecting this term, one can readily obtain the formula for Q_{max}^{TT} and write the stability condition in terms of the two inequalities: (45) for the vapor depth and

$$Q > Q_{max}^{TT} = \frac{40(1 + \eta_*^{-1} d_0^{-1})}{3\chi_* d_0^2 \left[160(1 + 4\eta_*^{-1} d_0^{-1})(l_{ca}/d_2)^2 (\delta_T/d_1)^3 - 1\right]} \tag{50}$$

for the heat flux. As was noted above, for the water system, the value of Q_{max}^{TT} calculated from the exact solution (34) is equal to 1.7×10^{-5}. Approximate formula (50) obtained using (40) (and ignoring the effect of the saturation-temperature perturbation) gives $Q_{max}^{TT} = 1.82 \times 10^{-5}$.

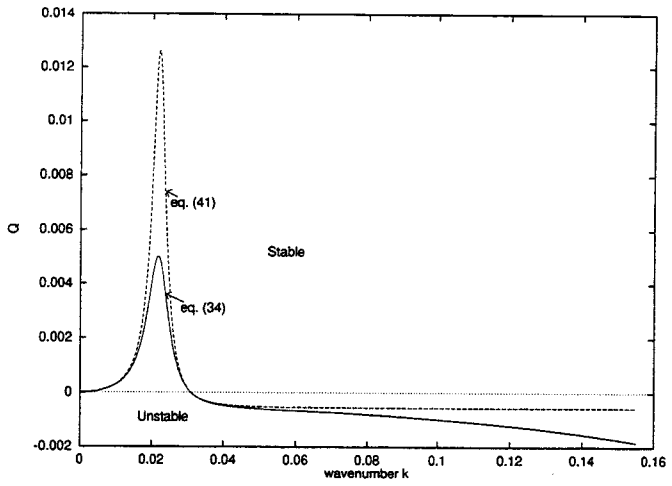

Figure 3: Comparison of the neutral curve with that one determined by the long-wave approximation (dashed curve) in the situation close to the criticality at which already three neutral curves exist. Both plates are isothermal; $d_1 = 7.8\times10^{-3}\,cm$, $d_0 = 20.51$ $N_g = 9.6\times10^{-4}$, $N_{cr} = 5.3\times10^{-5}$, $\tau_e = 9.9\times10^{-9}$. The values of ρ_*, η_*, χ_*, λ_* are the same as for figure 1.

Equations (42)–(44) are seen to be analogous to equation (41) just examined. Therefore, we present only the conditions of stability to nonoscillatory perturbations, predicted from the long-wave approximations in the case where requirements (40) are satisfied, $\tau_e = 0$, and $d_1 \ll d_2 \ll l_{ca}$. These conditions are:

$$\begin{cases} (d_1/\delta_q)^2(d_2/l_{ca})^2 < 160(1+4\eta_*^{-1}d_0^{-1}) \\ Q > Q_{max}^{qT} = \dfrac{40(1+\eta_*^{-1}d_0^{-1})}{3\chi_* d_0^2\,[160(1+4\eta_*^{-1}d_0^{-1})(l_{ca}/d_2)^2(\delta_q/d_1)^2-1]} \end{cases} \tag{51}$$

when at the lower wall the heat flux is constant and the upper wall is isothermal,

$$\begin{cases} (d_1/\delta_T)^3(d_2/l_{ca})^2 < 96(1+4\eta_*^{-1}d_0^{-1}) \\ Q > Q_{max}^{Tq} = \dfrac{8(1+\eta_*^{-1}d_0^{-1})}{\chi_* d_0^2\,[96(1+4\eta_*^{-1}d_0^{-1})(l_{ca}/d_2)^2(\delta_T/d_1)^3-1]} \end{cases} \tag{52}$$

when the lower wall is isothermal and the upper one is at a given heat flux,

$$\begin{cases} (d_1/\delta_q)^2(d_2/l_{ca}) < 24(1+4\eta_*^{-1}d_0^{-1}) \\ Q > Q_{max}^{qq} = \dfrac{8(1+\eta_*^{-1}d_0^{-1})}{\chi_* d_0^2\,[24(1+4\eta_*^{-1}d_0^{-1})(l_{ca}/d_2)(\delta_q/d_1)^2-1]} \end{cases} \tag{53}$$

in the case where each wall is kept at a constant heat flux. To the values Q_{max}^{Tq} and Q_{max}^{qT} there corresponds the wave number $k_m = \sqrt{N_g/2}$. The maximal value Q_{max}^{qq} is reached at $k = 0$. In (51) and (53),

$$\delta_q = \frac{\eta_1^{1/2}\chi_2^{1/2}}{[(\rho_2-\rho_1)g\sigma]^{1/4}} \tag{54}$$

is a characteristic length which, the same as the length δ_T, is a characteristic thickness for the vapor layer, at which the destabilizing gravity effect is already affected by the stabilizing effects of the vapor viscosity and of the liquid heat diffusivity. In contrast with the length δ_T involving in stability conditions (45), (50) and (52) for the arrangement with the isothermal lower plate,

the length δ_q pertains to the cases where the heat flux is constant at the wall contacting with the vapor layer. In condition (52), the term $\eta_*^{-1}d_0^{-1}$ that reflects a contribution of the liquid viscosity effect can be expressed through the lengths l_{ca}, δ_T with the help of (48), (49). In (51), (53), one can express the term $\eta_*^{-1}d_0^{-1}$ through the lengths l_{ca}, δ_q as follows

$$\eta_*^{-1}d_0^{-1} = V_q(d_1/\delta_q)(l_{ca}/d_2) \tag{55}$$

with the parameter

$$V_q = \frac{\eta_2}{\eta_1}\frac{\delta_q}{l_{ca}} = \frac{\eta_2\chi_2^{1/2}[(\rho_2-\rho_1)g]^{1/4}}{(\eta_1)^{1/2}\sigma^{3/4}} \tag{56}$$

characterizing the liquid viscosity effect. Note that for the water system, $\delta_q = 3\times 10^{-5}\,cm$. Note also that the thickness δ_q is related to δ_T by

$$\delta_q = \delta_T^{3/2}l_{ca}^{-1/2}. \tag{57}$$

In (50) - (53), the inequalities for Q contain terms $\chi_* d_0^2$ which also can be expressed through relative thicknesses d_1/δ_T (or d_1/δ_q), d_2/l_{ca} and the ratio δ_T/l_{ca} (or δ_q/l_{ca}). Furthermore, in conditions (51), (53) for which $q = const$ at the lower plate, the parameter $Q = qd_1/(\rho_1\chi_1 L)$ depends on d_1, and it can be replaced by $(d_1/\delta_q)\bar{Q}$ with $\bar{Q} = q\delta_q/(\rho_1\chi_1 L)$. We can say that stability conditions (45), (50), (52) or (51), (53) can be described in terms of the Bond number for liquid $N_g d_0^2 = (d_2/l_{ca})^2$, the gravity parameter

$$G_T = \left(\frac{d_1}{\delta_T}\right)^3 = \frac{(\rho_2-\rho_1)gd_1^3}{\rho_1\nu_1\chi_2}, \quad \text{or} \quad G_q = \left(\frac{d_1}{\delta_q}\right)^4 = \frac{(\rho_2-\rho_1)g\sigma d_1^4}{\rho_1^2\nu_1^2\chi_2^2}$$

for vapor, and the ratio δ_T/l_{ca} or δ_q/l_{ca} of the two characteristic lengths.

Assume that the lower plate is isothermal and that, given depths d_1, d_2, and a temperature difference $T_{1w} - T_0$, the stability condition (52) is satisfied. Then, direct comparison of (52) with condition (45), (50) shows that the latter one is also satisfied. This means that if the arrangement is stable to perturbations keeping at the upper plate a constant value of the heat flux, then it is also stable to perturbations under which, at this plate, a constant value is conserved for the temperature. This statement was confirmed by numerical calculations for the neutral stability made on base of equations (34), (36). The analogous statement is valid also in the case where at the lower plate a constant heat-flux condition is imposed (here, condition (51) was shown to follow from (53) under assumption $d_2 < 4l_{ca}$).

We compare now stability of the arrangements differing in the thermal conditions on the lower plate with the help of figures 4, 5 plotted for the depths as in figure 1, for which the arrangement with two isothermal plates was stable. Figures 4 and 5 correspond to the case where the lower plate is at a given heat flux. In figure 4, where the upper plate is isothermal, there exists inside the interval $(0, \sqrt{N_g})$ a wide domain of instability. In figure 5, for which the upper wall is at a given heat flux, the instability takes place in the whole interval $(0, \sqrt{N_g})$. This shows that, for the given d_1, d_2, configuration with the isothermal lower plate is the most stable. This result valid also for all configurations with $d_1 \ll d_2 \ll l_{ca}$ follows from that the ratios of the right-hand sides of (52), (45) to the right-hand sides of (51), (53) (equal respectively to d_1/l_{ca} and $d_1 d_2/l_{ca}^2$) are very small. Finally, note that the effect of the surface-temperature dependence versus pressures of the phases (parameter τ_e) on onset of nonoscillatory instability was studied numerically. Calculations for a critical dependence $Q(k)$ were performed using original neutral stability conditions (34) - (37) in a wide range of depths d_1, d_2, $d_1 \le d_2$, for

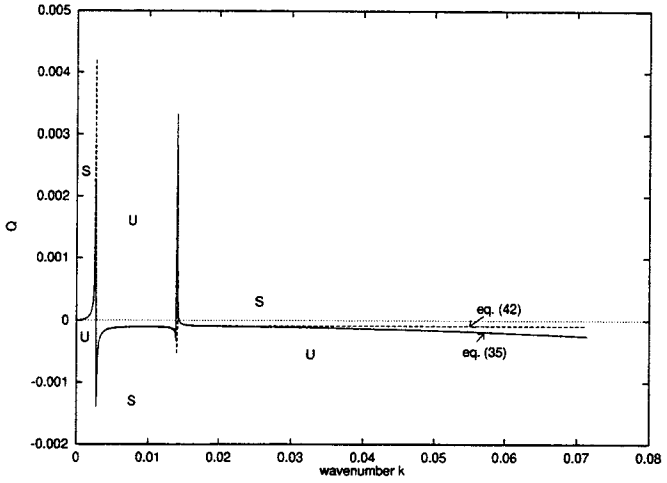

Figure 4: Neutral stability curves for the water system having the same parameters as in figure 1. The only difference from the situation to which figure 1 pertains is in that the lower plate is at a fixed heat flux rather then at a given temperature. In contrast with figure 1, a domain of instability exists for all positive Q.

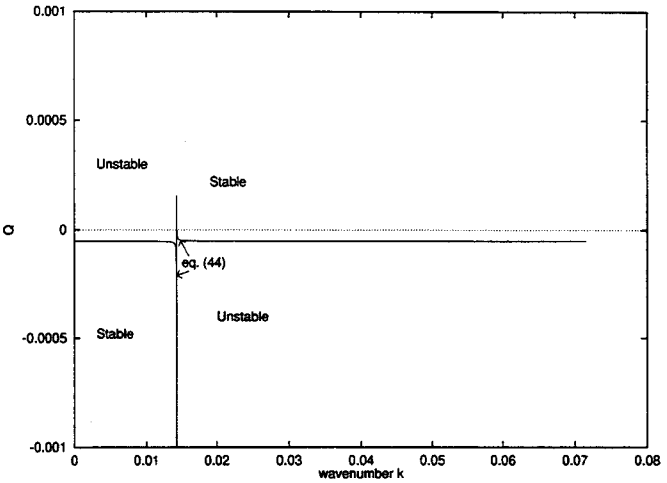

Figure 5: Neutral stability curves for long waves in the case both plates are at a fixed heat flux. The depth d_1 and the parameters d_0, N_g, N_{cr}, τ_e, ρ_*, η_*, χ_*, λ_* are as for figure 1. Figure shows that with any heating from the bottom, the instability interval is the same as in the case of two isothermal immiscible fluids.

which a one neutral stability curve exists. Very small depths d_1 were also considered. No influence of the parameter τ_e on neutral stability curves was found. Since the case $d_1 = d_2$ was also included, below, in analysis of the case of two layers with equal thicknesses we put $\tau_e = 0$.

Two layers of equal thickness

In the case when both phases have one and the same thickness ($d_1 = d_2 = d$), we obtain the long-wave approximations to (34)–(37) by assuming $\lambda_* \gg 1$, $\nu_* \gg 1$, $\rho_* \ll 1$, $\chi_* \gg 1$. In the limit $k \to 0$, keeping a first order approximation to each term in (34)–(37), we obtain from (34)–(36) the following common form

$$Q = Q(k, c_1, c_2) = -\frac{c_1(k^2 - N_g)[3\tau_e\lambda_*^{-1}(1 + 4\eta_*^{-1}) + k^2(1 + \eta_*^{-1})]}{3\chi_*[k^4 - N_g k^2 + c_2 N_{cr}\chi_*^{-1}(1 + 7\eta_*^{-1})]} \tag{58}$$

for the neutral stability condition. From (37), we obtain

$$Q = Q^{qq}(k) = -\frac{8(k^2 - N_g)[3\tau_e\lambda_*^{-1}(1 + 4\eta_*^{-1}) + 1 + \eta_*^{-1}]}{\chi_*[k^2 - N_g + 48N_{cr}\chi_*^{-1}(1 + 7\eta_*^{-1})]}. \tag{59}$$

In (58) and below we have $c_2 = 2c_1 = 80$ for the case where both plates are isothermal and $c_2 = c_1 = 40$ ($c_2 = c_1 = 24$) when the upper (lower) plate is isothermal and the lower (upper) one is at a given heat flux. Analysis of (58), (59) leads, under additional assumptions $7\eta_*^{-1} \gg 1$ and $\tau_e = 0$, to the nonoscillatory stability conditions

$$\begin{cases} d < d_{max}(c_2) = (28c_2)^{1/5}\delta, \\ Q > Q_{max}(c_1, c_2) = \frac{c_1(1+\eta_*^{-1})}{3\chi_*[(d_{max}(c_2)/d)^5 - 1]}, \end{cases} \tag{60}$$

and

$$\begin{cases} d_1 < d_{max}^{qq} = 336^{1/3}\delta_{qq}, \\ Q > Q_{max}^{qq} = \frac{8(1+\eta_*^{-1})}{\chi_*[(d_{max}^{qq}/d)^3 - 1]}, \end{cases} \tag{61}$$

respectively. In (60), (61)

$$\delta = \frac{\eta_2^{1/5}\chi_2^{1/5}\sigma^{1/5}}{[(\rho_2 - \rho_1)g]^{2/5}}, \qquad \delta_{qq} = \frac{\eta_2^{1/3}\chi_2^{1/3}}{[(\rho_2 - \rho_1)g]^{1/3}}. \tag{62}$$

For the test water system at earth gravity, $\delta = 0.013\,cm$, $\delta_{qq} = 1.7 \times 10^{-3}\,cm$. As is seen from (60) - (62), the stabilizing effects are viscosity and heat diffusivity of liquid.

The formulas

$$\delta = \frac{\delta_T}{\eta_*^{1/3}}\left(\frac{\eta_*^{1/3} l_{ca}}{\delta_T}\right)^{2/5} = (28c_2)^{1/5}\frac{\delta_q}{\eta_*^{1/2}}\left(\frac{\eta_*^{1/2} l_{ca}}{\delta_q}\right)^{3/5},$$

$$\delta_{qq} = 336^{1/3}\frac{\delta_q}{\eta_*^{1/2}}\left(\frac{\eta_*^{1/2} l_{ca}}{\delta_q}\right)^{1/3} = 336^{1/3}\frac{\delta_T}{\eta_*^{1/3}}$$

can be shown to be valid. They show that, in the case under consideration, for all four kinds of thermal boundary conditions the thin-layer effects can be described in terms of the thickness $\delta_T/\eta_*^{1/3}$ as well as in terms of $\delta_q/\eta_*^{1/2}$. Here, the ratio $\eta_*^{1/3} l_{ca}/\delta_T$ or $\eta_*^{1/2} l_{ca}/\delta_q$ appears as a dimensionless group characterizing the thin-layer effect. It is interesting to note that, in the case where the plates are at a given heat flux, it is possible to express the maximal depth d_{max}^{qq} in terms of

the thickness $\delta_T/\eta_*^{1/3}$ only. Also, one can use the capillary length l_{ca} as the characteristic length. In such a case one has $\delta = l_{ca}R^{1/5}$, $\delta_{qq} = l_{ca}R^{1/3}$, where

$$R = \eta_*^{-1}(\delta_T/l_{ca})^3 = \eta_*^{-1}(\delta_q/l_{ca})^2. \tag{63}$$

Equations (60)–(61) show that the critical values Q_{max}, Q_{max}^{qq} above which the arrangement is stable to nonoscillatory perturbations increase monotonically as the thickness d is increased. For the case of two isothermal plates, numerical calculations were performed on the base of general equation (34). The depths d was varied from $10^{-3}cm$ till the value $d_{max} = 0.052cm$ at which existence of a very thin interval of the instability has been found first. (Note, that the approximate formula (60) gives the maximal depth $d_{max} = 0.059cm$). The calculations confirm that, increasing the depth d, Q_{max}^{TT} grows monotonically. At small depths, the agreement between numerical and approximate values for Q_{max}, determined by (60), is very good. For $d = 5 \times 10^{-3}cm$, $10^{-2}cm$, and $d = 2 \times 10^{-2}cm$, both the numerical and approximate results give $Q_{max} = 1.16 \times 10^{-5}$, 3.7×10^{-4}, and 1.19×10^{-2}, respectively. To these values of Q_{max} there correspond respectively the following temperature differences $T_{1w} - T_0$: $0.013K$, $0.41K$, and $13.6K$. For $d = 3 \times 10^{-2}cm$ the numerical calculations give $Q_{max} = 9.6 \times 10^{-2}$, while the approximate formula (60) predicts that $Q_{max} = 9.37 \times 10^{-2}$. However, here the corresponding temperature differences are very large. For $Q_{max} = 9.6 \times 10^{-2}$, one has $T_{1w} - T_0 = 109K$.

Note finally, that one can put the question of stability in the following way. Given the heat flux number Q, under which values of the relative thickness d/d_{max} is the arrangement stable? To answer this question one has to resolve the last inequalities in (60), (61) with respect to d/d_{max}. Then (61) yields the stability condition $d/d_{max}^{qq} < \left(1 + 8(1 + \eta_*^{-1})/(\chi_* Q)\right)^{-1/3}$ for the case where the plates are at a constant heat flux. For the other three kinds of the thermal condition, from (60), follows the condition $d/d_{max}(c_2) < \left(1 + c_1(1 + \eta_*^{-1})/(\chi_* Q)\right)^{-1/5}$. As the number Q is increased, the right-hand sides of the last two inequalities increase. Thus, the larger Q, the arrangement is linearly stable to nonoscillatory perturbations in a more wide interval of the relative thickness.

Thin liquid layer

The asymptotic analysis for long waves now will be carried out under the assumption that the liquid layer is very much thinner than the vapor one. As above, the analysis is performed for systems whose physical parameters have the same orders of magnitudes as that for the test water system. We assume therefore

$$d_0 \ll 1, \quad \chi_*\rho_* < 1, \quad \eta_* < 1, \quad \chi_*\nu_*\rho_* = 0(1).$$

For simplicity we assume also $\nu_* d_0^2 \ll 1$. Then, at the limit $k \to 0$, $k_0 \to 0$, $(k \gg k_0)$, we obtain from (21), (22), and (38) the following approximate formulas

$$r \sim -\frac{3\rho_*}{2kd_0}, \quad G \sim \frac{3}{2k^3\nu_* d_0^3}, \quad H \sim \frac{3(4\nu_* d_0^3 + \rho_*)}{\nu_* d_0^3}.$$

Here the consideration will be made only for two kinds of the thermal boundary conditions. Namely, the lower plate is assumed to be isothermal while, at the upper plate, the heat-flux or the temperature condition is given. Equations (27) and (32) yield $F^{TT} = F^{Tq} \sim (3\rho_* + 14d_0)/(10d_0)$. Substituting these approximations into (34), (36), under the assumption $\lambda_*^{-1}d_0^{-1} \gg 1$, we obtain the following expressions

$$Q^{TT}(k) = -\frac{40(k^2 - N_g)[3\tau_e\lambda_*^{-1}d_0^{-1}(4\nu_* d_0^3 + \rho_*) + \nu_* d_0^3 k^2]}{\nu_* d_0^2(3\rho_* + 14d_0)\left[k^4 - N_g k^2 + 120N_{cr}\nu_*^{-1}d_0^{-3}(3\rho_* + 14d_0)^{-1}\right]},$$

$$Q^{Tq}(k) = -\frac{40(k^2 - N_g)[3\tau_e(4\nu_* d_0^3 + \rho_*) + \nu_* d_0^3 k^2]}{\nu_* d_0^2(3\rho_* + 14d_0)\left[k^4 - N_g k^2 + 120 N_{cr}\nu_*^{-1} d_0^{-2}(3\rho_* + 14d_0)^{-1}\right]}. \tag{64}$$

The functions Q^{TT} and Q^{Tq} are continuous when the polynomials in k^2 (in the denominators) allow no positive roots. This is expressed by the conditions

$$\nu_* d_0^3 N_g^2(\rho_* + 14d_0/3)/N_{cr} < 160, \quad \nu_* d_0^2(\rho_* + 14d_0/3)N_g^2/N_{cr} < 160, \tag{65}$$

respectively. These conditions can be written correspondingly as follows

$$\frac{14}{3}\frac{d_1}{l_{ca}}\left(\frac{d_2}{\delta_T'}\right)^4 + \left(\frac{d_1}{l_{ca}}\right)^2\left(\frac{d_2}{\delta_T''}\right)^3 < 160, \quad \frac{14}{3}\left(\frac{d_1}{l_{ca}}\right)^2\left(\frac{d_2}{\delta_q'}\right)^3 + \left(\frac{d_1}{l_{ca}}\right)^3\left(\frac{d_2}{\delta_q''}\right)^2 < 160, \tag{66}$$

where

$$\delta_T' = \frac{\rho_1^{1/4}\chi_1^{1/4}\nu_2^{1/4}\sigma^{1/8}}{[(\rho_2 - \rho_1)g]^{3/8}}, \quad \delta_q' = \frac{\rho_1^{1/3}\chi_1^{1/3}\nu_2^{1/3}}{[(\rho_2 - \rho_1)g]^{1/3}} \tag{67}$$

and

$$\delta_T'' = \frac{\eta_2^{1/3}\chi_1^{1/3}}{[(\rho_2 - \rho_1)g]^{1/3}} \quad \delta_q'' = \frac{\eta_2^{1/2}\chi_1^{1/2}}{[(\rho_2 - \rho_1)g\sigma]^{1/4}}.$$

In figure 6 the neutral curves defined by (34) are plotted for the two cases: $d_1 = 0.16cm$, $d_2 = 0.03cm$ and $d_1 = 0.16cm$, $d_2 = 0.01cm$. In the former case, the first condition (66) is not satisfied. There exist three neutral curves. Positive Q, the instability takes place in the domain above curve 2, located between curves 1 and 3. The interval of the unstable wave numbers is almost the same as the interval of the Rayleigh – Taylor instability. For the latter case, the first condition (66) is satisfied and there exists one neutral curve (curve 4) for which $Q_{max}^{TT} \approx 150$. Note that to the value $Q^{TT} = 1$ there corresponds the temperature difference $T_{1w} - T_0 = 1134.7K$. For physically realistic values of $T_{1w} - T_0$ the parameters Q are very small. Since the instability takes place below curve 4 and since the parameters Q are small, it appears that the instability interval practically coincides with the interval of the Rayleigh – Taylor instability.

This is visualized in figure 7 by curve 1, which is curve 4 from figure 6 plotted in a range of small Q. Curve 2 is plotted for $d_1 = 0.16\,cm$, $d_2 = 5 \times 10^{-4} cm$. To the maximal value $Q_{max}^{TT} = 3.5 \times 10^{-5}$ there corresponds $T_{1w} - T_0 = 0.039K$. Figures 5, 6 show that, given d_1, stable arrangements should have sufficiently small depths d_2. To describe the thin-layer effects, we find first the maximal values for the functions Q^{TT}, Q^{Tq}. Setting their first derivatives equal to zero, we obtain the equations

$$\begin{gathered}(2k^2 - N_g)\left(1 + \frac{\tau_e(4\nu_* d_0^2 + \rho_*/d_0)(3\rho_* + 14d_0)}{160\lambda_* N_{cr}}(3N_g - 2k^2)\right) + \\ \frac{3\tau_e(4\nu_* d_0^2 + \rho_*/d_0)}{\lambda_*\nu_* d_0^3}\left(1 - \frac{N_g^2\nu_* d_0^3(\rho_* + 14d_0/3)}{160N_{cr}}\right) = 0\end{gathered} \tag{68}$$

and

$$\begin{gathered}(2k^2 - N_g)\left(1 + \frac{\tau_e(4\nu_* d_0^2 + \rho_*/d_0)(3\rho_* + 14d_0)}{160N_{cr}}(3N_g - 2k^2)\right) - \\ \frac{3\tau_e(4\nu_* d_0^2 + \rho_*/d_0)}{\nu_* d_0^2}\left(1 - \frac{N_g^2\nu_* d_0^2(\rho_* + 14d_0/3)}{160N_{cr}}\right) = 0\end{gathered} \tag{69}$$

for unknown wave numbers k_m^{TT} and k_m^{Tq} at which the maximal values are reached.

Assume for simplicity $d_0 > \rho_*$. Let $k \in (0, \sqrt{N_g})$, then $0 < 3N_g - 2k^2 < 3N_g$ and the second term in the brackets multiplying $2k^2 - N_g$ can be shown to be much less than the first one when

$$3(4\nu_* d_0^2 + \rho_*/d_0)(3\rho_*/d_0 + 14)d_2 \ll 160\rho_1^2\chi_1 L^2/[T_0\lambda_2(\rho_2 - \rho_1)g]$$

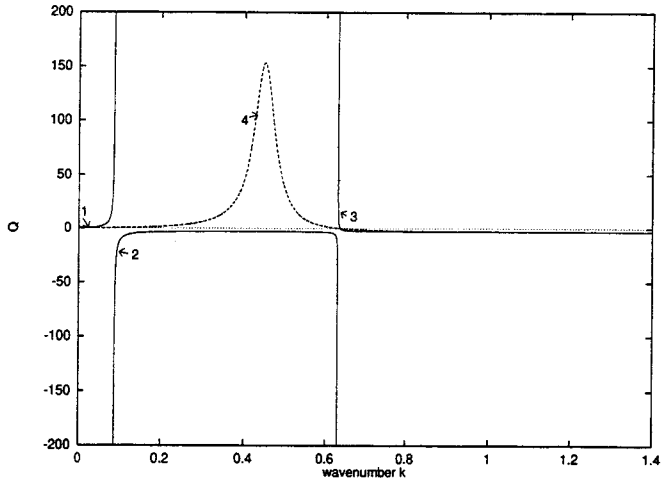

Figure 6: Neutral curves in the case the liquid layer is thinner than the vapor layer. Both plates are isothermal, $\rho_* = 6.2 \times 10^{-4}$, $\eta_* = 0.045$, $\chi_* = 118.69$, $\lambda_* = 0.035$. Vapor depth $d_1 = 0.16\,cm$, $N_g = 0.4$, $N_{cr} = 2.6 \times 10^{-6}$, $\tau_e = 2.4 \times 10^{-11}$. Curves 1, 2, and 3 are for the case $d_2 = 0.03\,cm$. Curve 4 corresponds to the case $d_2 = 0.01\,cm$.

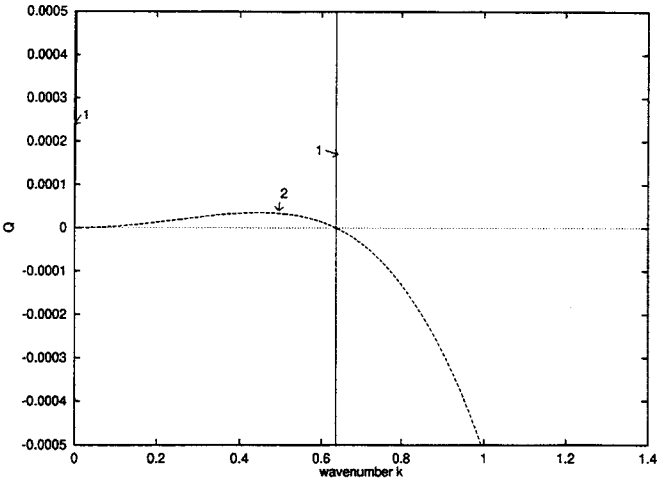

Figure 7: Neutral curves for the water system. Both plates are isothermal. Curve 1 is a part of curve 4 from figure 6, plotted in a range of small Q. Curve 2 is for $d_1 = 0.16\,cm$, $d_2 = 5 \times 10^{-4}\,cm$. The parameters ρ_*, η_*, χ_*, λ_* are as in the foregoing figures. The parameters N_g, N_{cr} and τ_e are as in figure 6.

for the former equation and when

$$3(4\nu_* d_0^2 + \rho_*/d_0)(3\rho_*/d_0 + 14)d_2 \ll 160\rho_1^2\chi_1 L^2/[T_0\lambda_1(\rho_2 - \rho_1)g]$$

for the latter one. Here, the quantities standing on the right-hand sides are equal, for the water system, to $1.46 \times 10^3\, cm$ and to $4.15 \times 10^4\, cm$ respectively. Hence they are very large and, under the above assumption $\nu_* d_0^2 \ll 1$, the inequalities are satisfied. Neglecting the terms just shown to be very small, we next estimate the ratio of the last terms on the right-hand side of (68), (69) to N_g in order to find conditions under which these terms can be neglected also. From (65), it follows that the absolute value of the terms standing in the large brackets is less than 2. Using this, we found that the corresponding ratios are very small in comparison with unity when

$$\frac{6(4\nu_* d_0^2 + \rho_*/d_0)T_0\lambda_2\nu_2\sigma}{\rho_1 L^2(\rho_2 - \rho_1)g d_1 d_2^3} \ll 1 \quad \text{or} \quad \frac{6(4\nu_* d_0^2 + \rho_*/d_0)T_0\lambda_1\nu_2\sigma}{\rho_1 L^2(\rho_2 - \rho_1)g d_1^2 d_2^2} \ll 1$$

for equations (68), (69) respectively. Since $\nu_* d_0^2 \ll 1$, the last inequalities are equivalent correspondingly to

$$d_2^3 d_1 > 30\frac{T_0\lambda_2\nu_2\sigma}{\rho_1 L^2(\rho_2 - \rho_1)g}, \qquad d_2^2 d_1^2 > \frac{T_0\lambda_1\nu_2\sigma}{\rho_1 L^2(\rho_2 - \rho_1)g}. \tag{70}$$

If we take $d_1 = 0.1\, cm$, then, for the water system, the first inequality is satisfied for $d_2 > 4.6^{1/3} \times 10^{-4}\, cm$ while the second one is valid for all $d_2 > \rho_* d_1 = 6 \times 10^{-5}\, cm$.

For the situation where conditions (70) are not satisfied, the effect of the surface temperature variation on the neutral stability was studied numerically. When the upper plate is at a given heat flux, we didn't find any influence of parameter τ_e. When it is isothermal, the most strong deviation of neutral curves was found for $d_1 = 0.02\, cm$ $d_2 = 10^{-5}\, cm$. Here, $\tau_e = 1.5 \times 10^{-9}$ and the value of $Q_{\max}^{TT}$ equal to 2.7×10^{-5} is about two times larger than the value 1.9×10^{-5} obtained for $\tau_e = 0$.

When conditions (70) are satisfied, in equations (68), (69) the terms proportional to τ_e can be neglected. Hence, $k_m^{TT} = k_m^{Tq} = N_g/2$. We find then

$$Q_{max}^{TT} = \frac{40 d_0}{3\left(\frac{160 N_{cr}}{\nu_* d_0^3 N_g^2} - \rho_* - 14 d_0/3\right)}, \qquad Q_{max}^{Tq} = \frac{40 d_0}{3\left(\frac{160 N_{cr}}{\nu_* d_0^2 N_g^2} - \rho_* - 14 d_0/3\right)}. \tag{71}$$

Assume Q is given. By using (71), the conditions of stability to nonoscillatory perturbations $Q > Q_{max}^{TT}$ and $Q > Q_{max}^{Tq}$ can be written correspondingly as

$$\frac{160 N_{cr}}{\nu_* d_0^4 N_g^2} > \frac{40}{3Q} + \frac{\rho_*}{d_0} + \frac{14}{3}, \qquad \frac{160 N_{cr}}{\nu_* d_0^3 N_g^2} > \frac{40}{3Q} + \frac{\rho_*}{d_0} + \frac{14}{3}. \tag{72}$$

For physically realistic values of the temperature differences $T_{1w} - T_0$, the values of Q are of order $10^{-4} - 10^{-2}$. Thus, on the right-hand sides of the stability conditions (72), the first term dominates. The conditions are then simplified to give $\nu_* d_0^4 N_g^2/N_{cr} < 12Q$ and $\nu_* d_0^3 N_g^2/N_{cr} < 12Q$. The latter conditions can be written in terms of the characteristic length scales (67) as follows:

$$\left(\frac{d_1}{l_{ca}}\right)\left(\frac{d_2}{\delta_T'}\right)^4 < 12Q$$

for the case where the upper plate is isothermal and

$$\left(\frac{d_1}{l_{ca}}\right)^2\left(\frac{d_2}{\delta_q'}\right)^3 < 12Q$$

where it is at a given heat flux.

7 Discussion and conclusions

We consider liquid and vapor layers having common interface and located between two parallel plates perpendicular to gravity. We assume either a heat flux transferred across the two-layer system or a temperature at one of the plates be given and constant. In the latter case, the other plate is assumed to be at a fixed temperature or at a fixed heat flux. The lighter vapor lies below and is hotter then the liquid. We use a "two-sided model" in which dynamic and heat transfer are considered in both layers and are coupled as a consequence of jump-balances of momentum and energy as well as balances between mass flux, tangential velocities, chemical potentials and temperatures holding at the interface of the phases. The main purpose is to study a stability of an equilibrium state in the case where both layers are thin. Therefore, the buoyancy effect is neglected and the phases are considered as incompressible viscous fluids.

In the equilibrium state, there is no mass transfer across the interface. But disturbances induce surface gravity waves, phase change and convection associated with them. At the disturbed interface, there is competition between destabilizing gravity and stabilizing capillary effects. The effects of viscous and thermal dissipation and the convective heat and energy transfer to the interface cause the interface-temperature perturbations. The interfacial temperature depends on the pressures of the phases. Therefore it changes also due the perturbations of the pressures. Their interaction is affected by the effect of phase transformation. Our aim is to examine influence of the mentioned physical effects on a stability of the equilibrium state.

Equations (34)–(37) represent the neutral stability conditions derived for common fluids and arbitrary depth of the layers. They are studied asymptotically in the case of two thin layers, in which we distinguish the following situations: the vapor layer is much thinner then the liquid layer, both layers have equal depths, the liquid layer is very thin compared with the vapor layer.

We study the first situation imposing only rather weak requirements on properties of the fluids, namely, we assume the coefficients of dynamic viscosity and of heat diffusivity of vapor be not very small compared with those for liquid. Analysis of equations (34)–(37) leads to closed-form expressions for conditions of linear nonoscillatory stability. The stability is treated as the thin-layer effect because it is possible only for very small vapor depth. The analysis show that the thin-layer effect can be described in terms of two characteristic length scales, one of which is the capillary length. The other length is not so universal as the capillary length in the sense that it is defined by different expressions ((46), (54)) in the cases differing in the thermal condition at the plate adjacent to the vapor. While the Bond number, defined in terms of the capillary length, characterizes the ratio of the capillary to gravity effects acting at the interface, the parameters G_T and G_q, defined with the help of the second length, measure the relative effect of liquid heat diffusivity and vapor viscosity versus gravity. It appears, that this relative effect depends on the kind of the thermal condition imposed on the lower plate. For small Bond numbers, the thin-layer effect exists only if the effects of liquid heat diffusivity and of vapor viscosity dominate in comparison with the effect of convection associated with gravity waves and the heat flux number is sufficiently large. We have found that in absence of the phase change, but in presence of the thermocapillary effect, the liquid diffusivity and vapor viscosity do not stabilize the arrangement. Instead, they increase the length of the instability interval in comparison with that for the isothermal case. Hence, the phase change is an important factor for stabilizing the arrangement to linear nonoscillatory perturbations. Numerical and asymptotic analysis show that the stabilization is possible even with extremely small heating from below.

Although the stability conditions were obtained in the long-wave approximation where it is required that both the liquid and vapor layers have a thickness small compared with the capillary

length, they have shown to be also efficient when the liquid depth is of the same order as the capillary length. This is seen from results presented in figures 1, 2, 4. Therefore, the parameters G_T, G_q characterize the thin layer effect for the case $d_2 \sim l_{ca}$ also. The analysis of the case $d_2 \gg l_{ca}$ was made by Badratinova, Colinet, Hennenberg & Legros (1966a,b). In their analysis for thin vapor layer below semi-infinite liquid, the parameters G_T and G_q were shown to characterize the stabilizing effects of dissipation in the cases of the isothermal plate and of the plate at a constant heat flux respectively. From the aforesaid, we conclude that the parameters G_T, G_q (the lengths δ_T, δ_q) pertain specifically to the case where the vapor layer is much thinner than the liquid layer (which can be thin, thick or infinitely deep).

When the thin liquid and vapor layers have the same thickness and the kinematic viscosity, heat diffusivity and thermal conductivity coefficients of the vapor are much greater than that of the liquid, the thin-layer effect have shown to exist for all four kinds of the thermal boundary conditions. In this case, the stabilizing effects are viscosity and thermal diffusivity of the liquid phase. A linear stability to nonoscillatory perturbations is only possible when viscous and thermal dissipation in the liquid layer are sufficiently strong to overcome convection induced by gravity waves. Since the liquid and vapor layers have the same thickness, the stability conditions (equations (60), (61)) are expressed in terms of only one characteristic thickness. This thickness (δ) was found to be one and the same in the three cases in which one of the plates is isothermal . But it differs from the thickness (δ_{qq}) being a characteristic one for the case of two plates at a constant heat flux (formula (62)). Here, it is worth to note that the thin-layer effect cannot be described in terms of the capillary length. If the thickness of the layers is measured by the capillary length, then, for all four kinds of the thermal boundary conditions, the effects of dissipation are presented by one and the same dimensionless parameter (formula (63)) characterizing the ratio of 'diffusive thickness' to the capillary length.

The asymptotic analysis yields a maximal depth d_{max} such that the arrangement with the fluid depth $d > d_{max}$ cannot be stable. The arrangement is stable when the relative depths d/d_{max} belongs to some interval I having the length less than unity. The competition of the stabilizing and destabilizing effects depends on the heat flux number. As the heat flux number grows, the interval I gets wider. Its length approaches unity only in the limit $Q \to \infty$.

In the third situation where the liquid layer is much thinner than the vapor one, consideration was restricted to the two cases differing only in a thermal condition at the plate adjacent to the liquid layer. The lower plate was assumed to be isothermal. A thin-layer effect with the mechanism analogous to that described in the first two situations is established. The basic imposed requirements are: vapor is less viscous, the ratio of vapor to liquid heat diffusivity multiplied by the ratio of vapor to liquid density is less than unity. For both studied cases, the stabilizing effects are found to be the liquid viscosity and the vapor heat diffusivity. This is seen from the formulas (67) determining the characteristic lengths in terms of which the stability conditions are formulated. In contrast with the two previous situations, dependence of the interfacial temperature versus the pressure of the fluids cannot be always neglected. With very small depths of the liquid layer, this effect can give considerable contribution into the values of the maximal heat flux above which the arrangement is stable.

Oscillatory modes of perturbations remain to be examined. For the situation where the liquid layer lies below, oscillatory instability due to the phase change was found by Huang & Joseph 1992 in the case of two isothermal plates. However, unstable configurations have shown to be absent for the arrangements with very thin liquid or very thin vapor layers.

8 Appendix A

Here, expressions for the functions in kz, appearing in equations (23), (24) and (29) are presented.

$$L_1(kz) = [(1+f_1)r - f_2^+](kz) + 1,$$
$$L_2(kz) = -(f_2^- r + 1 + f_1)(kz) - f_1 r + f_2^+,$$
$$L_3(kz) = [(1+f_{10})r + \rho_* f_{20}^+](kz) + \rho_*,$$
$$L_4(kz) = (f_{20}^- r - \rho_* - \rho_* f_{10})(kz) - f_{10} r - \rho_* f_{20}^+.$$

$$P_{2T}(kz) = P_2(kz) - \frac{\lambda_* \chi_* f_{10}}{4k}[(2 + k_0 \mathrm{coth} k_0)r + \rho_*(3\mathrm{coth}k_0 + k_0 + 3k_0^{-1})],$$
$$P_{4T}(kz) = P_4(kz) + 2N_{cr}k^2 G(k,k_0)\mathrm{coth}k_0/(k^2 - N_g)$$
$$- \frac{\chi_* f_{10}}{4k}[(2 + k_0 \mathrm{coth}k_0)r + \rho_*(3\mathrm{coth}k_0 + k_0 + 3k_0^{-1})],$$

$$P_1(kz) = \frac{\lambda_* \chi_*}{4k}\{[(1+3f_{10})r + 3\rho_* f_{20}^+](kz) - -(f_{20}^- r - \rho_* - \rho_* f_{10})(kz)^2\},$$
$$P_2(kz) = \frac{\lambda_* \chi_*}{4k}\{(f_{20}^- r - 3\rho_* - \rho_* f_{10})(kz) - [(1+f_{10})r + \rho_* f_{20}^+](kz)^2\},$$
$$P_3(kz) = \{[(1+3f_1)r - 3f_2^+](kz) + (f_2^- r + 1 + f_1)(kz)^2\}/(4k) - 2\frac{N_{cr}k^2}{k^2 - N_g}G(k,k_0),$$
$$P_4(kz) = Q^{-1} + \{\chi_*[(1+3f_{10})r + 3\rho_* f_{20}^+] - [(1+3f_1)r - 3f_2^+]$$
$$- (f_2^- r + 3 + f_1)(kz) - [(1+f_1)r - f_2^+](kz)^2\}/(4k).$$

$$P_{2q}(kz) = P_2(kz) - \frac{\lambda_* \chi_*}{4k}\{f_{10}(1 + k_0 \mathrm{tanh}k_0 + 2k_0^{-1}\mathrm{tanh}k_0)r$$
$$- \rho_*[(f_{30}+2)\mathrm{tanh}k_0 - 3f_{20}^+]\},$$
$$P_{4q}(kz) = P_4(kz) + 2N_{cr}k^2 G(k,k_0)\mathrm{tanh}k_0/(k^2 - N_g)$$
$$- \frac{\chi_*}{4k}\{f_{10}(1 + k_0\mathrm{tanh}k_0 + 2k_0^{-1}\mathrm{tanh}k_0)r - \rho_*[(f_{30}+2)\mathrm{tanh}k_0 - 3f_{20}^+]\}.$$

9 Appendix B

Consider the problem on instability of an equilibrium interface between two viscous, isothermal, capillary, immiscible fluids from which the more dense fluid is on top. If each fluid occupies a half plane, the interval of wave numbers with respect to which the equilibrium is unstable does not depend on viscosity (Chandrasekhar 1961). Disturbances with wave numbers $\alpha > \alpha_c = \sqrt{(\rho_2 - \rho_1)g/\sigma}$ are stabilized by surface tension. Unstable modes occur only for $0 \le \alpha \le \alpha_c$ (this result was derived in Chandrasekhar 1961 for fluids with equal kinematic viscosities).

The purpose here is to prove that the instability interval is also independent of viscosity when only one fluid is in a half plane while the other one is in a thin layer. This will be shown under the assumption that the dynamic viscosity for the lower fluid is much less than that for the upper one, i.e., $\eta_* << 1$.

Let l denote the thickness of the thin layer, so that $l = d_1$ or $l = d_2$ depending on whether the lower or the upper fluid is of finite thickness. We will use the scales l(length), ν_1/l(velocity), l^2/ν_1(pressure). In particular, the wave number α is expressed in dimensionless form as $k = \alpha l$.

The evolution of normal modes of perturbations is then described by the following equations. The equations of motion lead to

$$(D^2-k^2)(D^2-k^2-n)\psi_1=0, \quad (D^2-k^2)(D^2-k^2-\nu_* n)\psi_2=0 \tag{73}$$

in fluid 1 and in fluid 2 respectively. At the interface $z=0$, conditions of continuity for the tangential velocity and the kinematic condition give

$$D\psi_1=D\psi_2, \quad na=k\psi_1=k\psi_2 \tag{74}$$

and the balances of the normal and tangential stresses are

$$\begin{gathered}\eta_*^{-1}(D^2+k^2)\psi_2=(D^2+k^2)\psi_1, \\ [(1-\rho_*^{-1})n+3(1-\eta_*^{-1})k^2]D\psi_2+\eta_*^{-1}D^3\psi_2-D^3\psi_1-R_k a=0,\end{gathered} \tag{75}$$

where

$$R_k=k\frac{(\rho_2-\rho_1)gl^2/\sigma-k^2}{\rho_1\nu_1^2/\sigma l}.$$

The no-slip condition at the solid plate and the condition on the decay of the disturbance at $z\to\infty$ are

$$\psi_1=D\psi_1=0 \quad \text{at} \quad z=-1, \quad \psi_2=D\psi_2\to 0 \quad \text{at} \quad z\to\infty \tag{76}$$

in the case where the lower fluid is in a thin layer and

$$\psi_1=D\psi_1=0 \quad \text{at} \quad z\to-\infty, \quad \psi_2=D\psi_2\to 0 \quad \text{at} \quad z=1 \tag{77}$$

if the upper fluid is in a thin layer.

Derive first the dispersion relation for the eigenvalue problem (73)–(76). The general solution of equations (73) can be expressed as

$$\begin{gathered}\psi_2=E^1\exp(-kz)+E^2\exp(-sz), \\ \psi_1=E^3\sinh kz+E^4\cosh kz+E^5\sinh s_1 z+E^6\cosh s_1 z\end{gathered} \tag{78}$$

where

$$s=\sqrt{k^2+\nu_* n}, \quad s_1=\sqrt{k^2+n} \quad (Re\, s>0). \tag{79}$$

Substituting (78) into the interfacial and boundary conditions, we are led to a system of linear algebraic equations with respect to unknown coefficients E^j $(j=1,2,..,6)$ and the interfacial wave amplitude a. From the kinematic condition it follows that $a=k(E^1+E^2+E^4+E^6)/(2n)$. With use of this expression, the amplitude a is excluded. Then, the system can be presented in the form:

$$\begin{aligned}kE^1+sE^2+kE^3+s_1E^5 &= 0, \\ E^1+E^2-E^4-E^6 &= 0, \\ 2\eta_*^{-1}k^2E^1+\eta_*^{-1}(k^2+s^2)E^2-2k^2E^4-(k^2+s_1^2)E^6 &= 0, \\ \tilde{R}(E^1+E^2+E^4+E^6)+\rho_*^{-1}nkE^1+nkE^3+ & \\ +(1-\eta_*^{-1})k^2(kE^3+s_1E^5-kE^1-sE^2) &= 0, \\ -E^3\sinh k+E^4\cosh k-E^5\sinh s_1+E^6\cosh s_1 &= 0, \\ kE^3\cosh k+s_1E^5\cosh s_1-kE^4\sinh k-s_1E^6\sinh s_1 &= 0.\end{aligned} \tag{80}$$

where $\tilde{R}=-R_k k/(2n)$.

We use the assumption $1 \ll \eta_*^{-1}$ and write down the determinant of the system. Then, we convert the determinant into a 3×3 one, applying for this the following transformations:

$$
\begin{aligned}
t_1 &= \{\|_2 - \|_1 \mapsto \|_2\,; \quad \|_4 + \|_1 \mapsto \|_4\,; \quad \|_6 - \|_4 \mapsto \|_6\,; \quad -\|_5 \mapsto \|_5\} \\
t_2 &= \{\|_1 + \|_4 \mapsto \|_1\,; \quad \|_2 + \|_4 \mapsto \|_2\,; \quad \|_3 + k\|_4 \mapsto \|_3 \quad (\eta_*^{-1} >> 1)\} \\
t_3 &= \{\rho_*^{-1}\|_4 + \|_1 \mapsto \|_1\,; \quad 2\eta_*^{-1}k^2\|_4 + n\|_3 \mapsto \|_3\}\,.
\end{aligned}
$$

The transformations t_i describe algebraic operations with columns, $\|_j$ denotes the column j, and the symbol $\mapsto$ shows to which column the result of the operation is placed. With the help of the described transformation, the conversion procedure can be presented as follows:

$$
\begin{vmatrix}
k & s & k & 0 & s_1 & 0 \\
1 & 1 & 0 & -1 & 0 & -1 \\
2\eta_*^{-1}k^2 & 2\eta_*^{-1}k^2 + \rho_*^{-1}n & 0 & -2k^2 & 0 & -2k^2 - n \\
\tilde{R} + \eta_*^{-1}ks^2 & \tilde{R} + \eta_*^{-1}k^2 s & nk - \eta_*^{-1}k^3 & \tilde{R} & -\eta_*^{-1}k^2 s_1 & \tilde{R} \\
0 & 0 & -\sinh k & \cosh k & -\sinh s_1 & \cosh s_1 \\
0 & 0 & k\cosh k & -k\sinh k & s_1\cosh s_1 & -s_1\sinh s_1
\end{vmatrix}
\xrightarrow{t_1}
$$

$$
s_1 k(s-k)
\begin{vmatrix}
1 & 1 & k & -1 & 0 \\
\eta_*^{-1}(s+k) & 0 & 2(\eta_*^{-1}-1)k^2 & 0 & k^2 - s_1^2 \\
-\eta_*^{-1}ks & n - \eta_*^{-1}k^2 & 2\tilde{R} + \eta_*^{-1}ks^2 & \eta_*^{-1}k^2 & 0 \\
0 & -k^{-1}\sinh k & \cosh k & s_1^{-1}\sinh s_1 & \cosh s_1 - \\
 & & & & -\cosh k \\
0 & \cosh k & -k\sinh k & -\cosh s_1 & k\sinh k - \\
 & & & & -s_1\sinh s_1
\end{vmatrix}
\xrightarrow{t_2}
$$

$$
s_1 k
\begin{vmatrix}
\rho_*^{-1}n & 0 & 2\eta_*^{-1}k^2 & -n \\
2\eta_*^{-1}k^2(s-k) - & n & 2\tilde{R} + & 0 \\
-\rho_*^{-1}nk & & +2\eta_*^{-1}k^3 + \rho_*^{-1}nk & \\
(s-k)s_1^{-1}\sinh s_1 & s_1^{-1}\sinh s_1 - & \cosh k + & \cosh s_1 - \\
 & -k^{-1}\sinh k & +ks_1^{-1}\sinh s_1 & -\cosh k \\
-(s-k)\cosh s_1 & \cosh k - & -k\sinh k - & k\sinh k - \\
 & -\cosh s_1 & -k\cosh s_1 & -s_1\sinh s_1
\end{vmatrix}
\xrightarrow{t_3}
$$

$$s_1 nk \begin{vmatrix} 2\eta_*^{-1}k^2(s-k) - \rho_*^{-1}nk & n & -R_k k + (2\eta_*^{-1}k^2 + \rho_*^{-1}n)nk \\ (s-k)s_1^{-1}\sinh s_1 + & s_1^{-1}\sinh s_1 - & (\cosh k + k s_1^{-1}\sinh s_1)n + \\ +\rho_*^{-1}(\cosh s_1 - \cosh k) & -k^{-1}\sinh k & +2\eta_*^{-1}k^2(\cosh s_1 - \cosh k) \\ -(s-k)\cosh s_1 + & \cosh k - & -(\sinh k + \cosh s_1)nk + \\ +\rho_*^{-1}(k\sinh k - s_1 \sinh s_1) & -\cosh s_1 & +2\eta_*^{-1}k^2(k\sinh k - s_1\sinh s_1) \end{vmatrix}$$

Setting the latter determinant equal to zero, we obtain the dispersion relation $F_1(n,k) = 0$ which determines, in the case where the lower fluid has a finite thickness, eigenvalues n as functions of the wave number k. The next step is to simplify the function $F_1(n,k)$, assuming the thickness of the lower fluid to be thin. In the limit $k \to 0$, the equation $F_1(n,k) = 0$ is reduced to the equality $n_0^{3/2}(\nu_*^{1/2}\cosh\sqrt{n_0} + \rho_*^{-1}\sinh\sqrt{n_0}) = 0$ with $n_0 = \lim_{k\to 0} n$. Since this equality can be satisfied only at $n_0 = 0$, it follows that $\lim_{k\to 0} n = 0$ and hence $\lim_{k\to 0} s_1 = 0$. Therefore, all hyperbolic functions appearing in the latter determinant can be approximated by their Taylor series. Then, the dispersion relation can be presented as follows:

$$F_1(n,k) \approx \begin{vmatrix} 2\eta_*^{-1}k^2(s-k) - & n & -R_k k + \\ -\rho_*^{-1}nk & & +(2\eta_*^{-1}k^2 + \rho_*^{-1}n)nk \\ (s-k) + 2^{-1}\rho_*^{-1}n & 6^{-1}n & n + \eta_*^{-1}k^2 n \\ -(s-k) - \rho_*^{-1}n & -2^{-1}n & -nk - 2\eta_*^{-1}k^2 n \end{vmatrix} = 0.$$

The obtained equation can be further reduced to the (n,k) -relationship

$$n\left(\rho_*^{-1}nk + 12 - \frac{36}{\eta_*^{-1}(s+k)+4}\right) - R_k k = 0 \tag{81}$$

valid under the assumption $\eta_*^{-1}k^2 = O(k) \ll 1$.

In equation (81), $n = 0$ corresponds to the value $R_k = 0$ which, in turn, is reached at $k = 0$ and at $k = k_c = \sqrt{(\rho_2 - \rho_1)g/\sigma}\, l$. Show now that, at $k > k_c$ the problem under consideration allows only damped modes. For this purpose, rewrite equation (81) in the form:

$$\eta_*^{-1}s = -4 - \eta_*^{-1}k + \frac{36}{-R_k k/n + \rho_*^{-1}nk + 12} \tag{82}$$

and prove that it does not allow any solution with a positive real part. Suppose such a solution exists, so that (82) is satisfied for a certain n for which $\mathrm{Re}n > 0$. Consider first the last term in (82). It can be presented as $36(A - iB)/(A^2 + B^2)$ where $A = -R_k k\mathrm{Re}n/[(\mathrm{Re}n)^2 + (\mathrm{Im}n^2)] + \rho_*^{-1}k\mathrm{Re}n + 12$, and $B = R_k k\mathrm{Im}n/[(\mathrm{Re}n)^2 + (\mathrm{Im}n^2)] + \rho_*^{-1}k\mathrm{Im}n$ are correspondingly the real and imaginary parts of the denominator. If $k > k_c$, one has $-R_k > 0$. Hence, with $\mathrm{Re}n > 0$, $A \geq 12$ and $36A/(A^2 + B^2) \leq 36/A \leq 3$. Then, from (82), using the obtained estimation for the real part of the last term, we find that $\mathrm{Re}s \leq -1 - \eta_*^{-1}k < 0$. Since in (78), (79) $\mathrm{Re}s$ is greater than zero, it is clear that, at $k > k_c$, all roots of equation (81) will have a negative real part. This means that, as in the case of two semi-infinite fluids, unstable modes occur only in the interval $0 < \alpha < \alpha_c$ whose length is independent of viscosity.

It follows also that, in the case under consideration, all unstable modes grow monotonically. Indeed, in the instability interval $0 < k < k_c$, the parameter R_k is positive and, from the above expression for B, it is readily seen that $\mathrm{sign}(B) = \mathrm{sign}(\mathrm{Im}n)$. In (82), the sign of imaginary part of

the right-hand side is opposite to the sign B and, consequently, to the sign of Imn. The imaginary part of the left-hand side has, however, the same sign as sign(Imn) because sign(Imn) = sign(Ims^2) and sign(Ims^2) = sign(Ims). The latter equality is valid for all complex numbers s with positive real part.

For the problem with the thin upper layer, the dispersion relation can be found in the same way. The solution to equations (73)–(75), (77) is now

$$\begin{aligned} \psi_1 &= D^1 \exp(kz) + D^2 \exp(s_1 z), \\ \psi_2 &= D^3 \sinh kz + D^4 \cosh kz + D^5 \sinh sz + D^6 \cosh sz \end{aligned} \tag{83}$$

where s_1 and s are determined by (79), $a = k(D^1 + D^2 + D^4 + D^6)/(2n)$ and the coefficients D^J satisfy the system of equations:

$$\begin{aligned} -kD^1 - s_1 D^2 + kD^3 + sD^5 &= 0, \\ D^1 + D^2 - D^4 - D^6 &= 0, \\ 2k^2 D^1 + (k^2 + s_1^2)D^2 - 2\eta_*^{-1} k^2 D^4 - \eta_*^{-1}(k^2 + s^2)D^6 &= 0, \\ \tilde{R}(D^1 + D^2 + D^4 + D^6) + nkD^1 - \rho_*^{-1} nkD^3 + & \\ +(1 - \eta_*^{-1})k^2(kD^1 + s_1 D^2 + kD^3 + sD^5) &= 0, \\ D^3 \sinh k + D^4 \cosh k + D^5 \sinh s + D^6 \cosh s &= 0, \\ kD^3 \cosh k + sD^5 \cosh s + kD^4 \sinh k + sD^6 \sinh s &= 0. \end{aligned} \tag{84}$$

By use of equivalent transformations, under the assumption $\eta_*^{-1} >> 1$, the determinant of the system (84) is reduced to the following one:

$$\begin{vmatrix} \rho_*^{-1}[2\eta_*^{-1}k^2(k - s_1) - nk] & -\rho_*^{-1} n & -R_k k - (2\eta_*^{-1}k^2 - n)nk \\ \rho_*^{-1}(s_1 - k)s^{-1}\sinh s - & k^{-1}\sinh k - & (\cosh k + ks^{-1}\sinh s)n + \\ -(\cosh k - \cosh s) & -s^{-1}\sinh s & +2\nu_*^{-1}k^2(\cosh k - \cosh s) \\ \rho_*^{-1}(s_1 - k)\cosh s - & \cosh k - & (\sinh k + \cosh s)nk + \\ -(k\sinh k - s\sinh s) & -\cosh s & +2\nu_*^{-1}k^2(k\sinh k - s\sinh s) \end{vmatrix}$$

Setting this determinant equal to zero, we obtain the dispersion relation $F_2(n,k) = 0$ and show first that, at the limit $k \to 0$, its solution n tends to zero. This also implies $\lim_{k\to 0} s = 0$. We expand next the hyperbolic functions into powers of theirs variables. Then, keeping the leading order terms, we get the approximation to the dispersion relation

$$F_2(n,k) \approx \begin{vmatrix} -\eta_*^{-1}k[2\eta_*^{-1}k(s_1 - k) + n] & \eta_*^{-1} n & -R_k k - \\ & & -(2\eta_*^{-1}k^2 - n)nk \\ \eta_*^{-1}(s_1 - k) + 2^{-1}n & 6^{-1}n & n \\ \eta_*^{-1}(s_1 - k) + n & 2^{-1}n & nk \end{vmatrix} = 0$$

which, for $k \ll 1$, is reduced to equation

$$n(nk + 12\eta_*^{-1} - \frac{36\eta_*^{-2}}{s_1 + 4\eta_*^{-1}}) - R_k k = 0.$$

Analyzing this equation similar to the former case, we prove that, in the case under consideration, all unstable perturbations grow monotonically and that they have wave numbers belonging to the interval $(0, k_c)$. All perturbations with wave numbers lying outside this interval are stable. For them, the growth rate n has the negative real part. The dimensional critical wave number α_c is the same as in the case of two semi-infinite fluids.

Acknowledgment

The work was supported by the Bundesministerium für Forschung und Technologie through the Otto-Benecke Stiftung in Bonn. The author is especially grateful to Prof. Dr. D. Kröner for his attention to this subject and the invitation to the Institute of Applied Mathematics at the Freiburg University. The author is very grateful to Dr. W. Dörfler for discussions of the manuscript and many useful remarks.

REFERENCES

BADRATINOVA, L.G. 1996 On crisis of transition from nucleate to film boiling. (In Russian)*Dinamika Sploshnoi Sredy* **111**, 15–20.

BADRATINOVA, L.G., COLINET, P., HENNENBERG, M.& LEGROS, J.C. 1996a Theoretical models for boiling at microgravity. In *Lecture Notes in Physics* (ed. L. Ratke, W. Walter & B. Feuerbacher) **464**, pp. 361–370 Springer Verlag, Berlin.

BADRATINOVA, L.G., COLINET, P., HENNENBERG, M.& LEGROS, J.C. 1996b On Rayleigh–Taylor instability in heated liquid-gas and liquid-vapor systems. *Russian J. Engnrg Thermophys.* **6**, 1–31.

BUSSE F.H., & SCHUBERT G. 1971 Convection in a fluid with two phases. *J. Fluid Mech.* **46**, 801–812.

CHANDRASEKHAR, S. 1961 *Hydrodynamic and hydromagnetic stability.* Clarendon Press, Oxford.

DELHAYE, J.M. 1974 Jump conditions and entropy sources in two- phase systems. Local instant formation. *Int. J. Multiphase Flow* **1**, 397–403.

DHIR, V., & LIENHARD, J. 1972 Discussion. *J. Basic Engrng., Trans. ASME, Series D* **94**, 160–162.

HSIEH, D.Y. 1972 Effects of heat and mass transfer on Rayleigh – Taylor Instability. *J. Basic Engrng., Trans. ASME, Series D* **94**, 156–160.

HUANG, A. & JOSEPH, D.D. 1992 Instability of the equilibrium of a liquid below its vapour between horizontal heated plate. *J. Fluid Mech.* **242**, 235–247.

HOOPER, A.P. 1985 Long-wave instability at the interface between two viscous fluids: thin layer effects. *Phys. Fluids* **28**, 1613–1618.

JOSEPH, D.D. & RENARDY Y. 1992 *Fundamentals of two-fluid dynamics. Part I: Mathematical theory and applications* Springer Verlag.

KULL, H., J. 1991 Theory of the Rayleigh – Taylor instability. *Phys. Rep.* **206**, 197–325.

STEPHAN, K. 1992 *Heat transfer in condensation and boiling.* Springer Verlag, Berlin.

PRIGOGINE, I.& DEFAY, R. 1973 *Chemical Thermodynamics.* Longman, London.

RAYLEIGH, LORD 1900 Investigation of the character of the equilibrium of an incompressible heavy fluid of variable density. *Scientific papers* **ii** Cambridge, England 200–207.

RENARDY, Y. 1985 Instability at the interface between two shearing fluids in a channel. *Phys. Fluids* **28**, 3441–3443.

RENARDY, Y. 1986 Interfacial stability in a two-layer Bénard problem. *Phys. Fluids* **29**, 356–363.

RENARDY, Y. 1987 The thin-layer effect and interfacial stability in a two-layer Couette flow with similar liquids. *Phys. Fluids* **30**, 1627–1637.

TAYLOR, G.I. 1950 The instability of liquid surfaces when accelerated in direction perpendicular to their plane. *Proc. Roy. Soc.* London **A 201**, 192–196.

[98–03] D. Hug: *Absolute continuity for curvature measures of convex sets II*

[98–04] D. Hilhorst, R. Schätzle: *The ono-phase Stefan problem as a limit of some two-phase Stefan problems*

[98–05] D. Hilhorst, L. A. Peletier, R. Schätzle: *Γ-Limit for the Extended Fisher-Kolmogorov equation*

[98–06] J. Spilker: *Die Fastperiodizität der Watson-Funktion*

[98–07] M. Peter: *A lattice point problem associated with two polynomials*

[98–08] M. Peter: *The local contribution of zeros of curvature to lattice point asymptotics*

[98–09] E. Bänsch, B. Höhn: *Numerical treatment of the Navier-Stokes equations with slip boundary condition*

[98–10] D. Wolke: *On some Dirichlet series related to the Riemann zeta function I,II*

[98–11] K. F. Siburg: *A dynamical systems approach to Birkhoff's Theorem*

[98–12] K. F. Siburg: *Aubry-Mather theory and the inverse spectral problem for planar convex domains*

[98–13] G. Dziuk: *Discrete anisotropic curve shortening flow*

[98–14] J. Becker, M. Rumpf: *Visualization of time-dependent velocity fields by texture transport*

[98–15] V. Bangert: *Minimal measures and minimizing closed normal one-currents*

[98–16] S. Goette: *Equivariant η-Invariants and η-Forms*

[98–17] A. Schmidt, K. G. Siebert: *Concepts of the finite element toolbox ALBERT*

[98–18] C. Bär: *Zero sets of semilinear elliptic systems of first order*

[98–19] A. Egelja, D. Kröner, R. Schwörer, N. Lanson, M. Mancip, J. P. Vila: *Combined finite volume and smoothed particle method*

[98–20] H. Witting: *Nichtparametrische Statistik: Aspekte ihrer Entwicklung 1957 - 1997*

[98–21] D. Hug, G. Last: *On support measures in Minkowski spaces and contact distributions in stochastic geometry*

[98–22] F. Auer: *Homologically versus homotopically area minimizing surfaces in 3-manifolds*

[98–23] S. Goette: *Equivariant η-invariants on homogeneous spaces*

[98–24] W. Dörfler: *Uniform a priori estimates for singularly perturbed elliptic equations in multi-dimensions*

[98–25] W. Dörfler: *Uniform error estimates for an exponentially fitted finite element method for singularly perturbed elliptic equations*

[98–26] L. Badratinova: *Thin-layer effects in a stability problem for equilibrium states between liquid and vapor*